

Gated Integration of Low-Rank Adaptation for Continual Learning of Language Models

Yan-Shuo Liang and Wu-Jun Li*

National Key Laboratory for Novel Software Technology,
Department of Computer Science and Technology, Nanjing University, P. R. China
liangys@smail.nju.edu.cn, liwujun@nju.edu.cn

Abstract

Continual learning (CL), which requires the model to learn multiple tasks sequentially, is crucial for language models (LMs). Recently, low-rank adaptation (LoRA), one of the most representative parameter-efficient fine-tuning (PEFT) methods, has gained increasing attention in CL of LMs. However, most existing CL methods based on LoRA typically expand a new LoRA branch to learn each new task and force the new and old LoRA branches to contribute equally to old tasks, potentially leading to forgetting. In this work, we propose a new method, called gated integration of low-rank adaptation (GainLoRA), for CL of LMs. GainLoRA expands a new LoRA branch for each new task and introduces gating modules to integrate the new and old LoRA branches. Furthermore, GainLoRA leverages the new gating module to minimize the contribution from the new LoRA branch to old tasks, effectively mitigating forgetting and improving the model’s overall performance. Experimental results on CL benchmarks demonstrate that GainLoRA outperforms existing state-of-the-art methods. Code is available at <https://github.com/liangyanshuo/gainlora>.

1 Introduction

Continual learning (CL), which requires the model to learn multiple tasks sequentially, is crucial for language models (LMs) [45]. Specifically, with extensive pre-trained knowledge and further fine-tuning strategies, existing LMs have demonstrated strong performance for a wide range of tasks [3, 7, 50, 51, 69]. However, when learning multiple tasks sequentially, LMs may lose knowledge acquired from old tasks, resulting in a significant degradation in performance on old tasks. This phenomenon, known as catastrophic forgetting [34, 38, 55, 57], highlights the need for developing effective CL methods for LMs. Existing CL methods can be categorized into two main categories. The first category [42] assumes that task identities are available during inference, while the second category [30, 71] tackles a more difficult and practical setting where task identities are unavailable during inference.

Recently, low-rank adaptation (LoRA) [19], one of the most representative parameter-efficient fine-tuning (PEFT) methods, has gained increasing attention in the CL of LMs [2, 57]. Specifically, by reparameterizing pre-trained weights in a low-rank form, LoRA updates only a limited number of parameters to adapt LMs to a downstream task, making the fine-tuning process much more efficient than updating all parameters of LMs [15]. This efficiency also benefits CL, making LoRA increasingly popular in CL of LMs.

Most existing CL methods based on LoRA [30, 71] typically expand a new LoRA branch for learning each new task while freezing all old LoRA branches. In this way, they avoid forgetting caused by

*Wu-Jun Li is the corresponding author.

directly updating the LoRA parameters of old tasks. However, to handle the practical CL scenario where task identities are unavailable at inference time, existing methods [30, 47, 57] based on LoRA integrate new and old LoRA branches through a simple addition. Consequently, they force the new and old LoRA branches to contribute equally to old tasks, which means that the new LoRA branch may cause a relatively large change in the model’s output on old tasks. This leads to forgetting and degrades the model’s overall performance in CL.

In this work, we propose a new method, called gated integration of low-rank adaptation (GainLoRA), for CL of LMs. The contributions of GainLoRA are listed as follows:

- GainLoRA expands a new LoRA branch to learn each new task and introduces gating modules to integrate the new and old LoRA branches.
- GainLoRA leverages the new gating module to minimize the contribution from the new LoRA branch to old tasks, effectively mitigating forgetting and improving the model’s overall performance.
- Experimental results on CL benchmarks show that GainLoRA outperforms existing state-of-the-art CL methods.

2 Related Work and Preliminaries

2.1 Related Work

Parameter-Efficient Fine-Tuning Parameter-efficient fine-tuning (PEFT) methods tune a limited number of parameters to adapt a pre-trained model for downstream tasks, showing much more efficiency than tuning all the parameters of the pre-trained model, especially for LMs [68]. For example, Adapter [18] modifies the model architecture by introducing trainable modules into Transformer layers and tunes these modules for downstream tasks. Prompt-tuning [24] and Prefix-tuning [25] insert learnable tokens into the input and tune them for downstream tasks. Low-rank adaptation (LoRA) [19] reparameterizes the original model parameters with low-rank matrices and tunes these matrices for downstream tasks. Although tuning significantly fewer parameters than full fine-tuning, PEFT can achieve comparable performance to full fine-tuning across a wide range of natural language processing (NLP) tasks [14, 19, 35, 66].

Continual Learning There are three main types of CL methods, categorized as regularization-based methods, memory-based methods, and expansion-based methods. Regularization-based methods [21, 22, 27] incorporate a regularization term to mitigate catastrophic forgetting. Memory-based methods [9, 29, 32, 49, 71] utilize memory mechanisms to preserve knowledge from old tasks. Expansion-based methods [20, 26, 28, 43] mitigate catastrophic forgetting by introducing new parameters for learning new tasks while typically freezing old parameters.

Many CL methods [1, 27, 28] are designed to train models from scratch. Recent studies [30, 42, 57, 63] have shown that leveraging PEFT strategies to fine-tune pre-trained models enables CL methods to achieve superior performance across tasks. Among various PEFT methods, LoRA has gained particular attention due to its strong performance and efficiency [30, 46, 57, 71]. However, most of these methods expand a new LoRA branch to handle each new task while freezing old LoRA branches to mitigate catastrophic forgetting. However, they force the new and old LoRA branches to contribute equally to old tasks, potentially leading to forgetting.

2.2 Preliminaries

Problem Definition We follow existing CL works [57, 71] to formalize the problem definition for CL of LMs. Specifically, in CL, a sequence of tasks $\{\mathcal{T}_1, \mathcal{T}_2, \dots, \mathcal{T}_T\}$ is presented to the model sequentially, where T denotes the total number of tasks. The t -th task \mathcal{T}_t consists of a training dataset \mathcal{D}_t . For any given sample $(\mathbf{x}_t, \mathbf{y}_t) \in \mathcal{D}_t$, \mathbf{x}_t denotes an input sentence and \mathbf{y}_t denotes the corresponding output. When learning the t -th new task, the model is required to mitigate catastrophic forgetting of the $t - 1$ previously learned tasks.

Similar to existing CL works for LMs [2, 71], we consider a more challenging CL setting defined by three key challenges: (1) the model is presented with a sequence of tasks spanning various types, such as dialogue generation, information extraction and so on; (2) the model is not provided with task

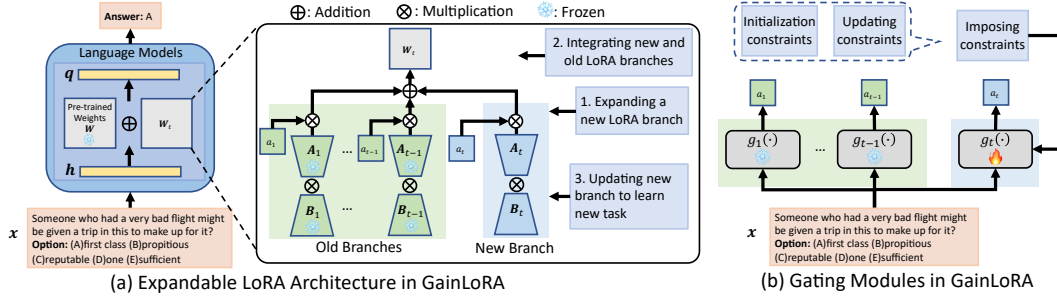


Figure 1: (a) shows the expandable LoRA architecture of our GainLoRA for learning the t -th new task. (b) shows that for each task \mathcal{T}_i , GainLoRA uses an independent gating module $g_i(\cdot)$ to generate integration coefficient a_i .

identities at inference time; (3) the model must learn without access to real or synthetic samples from previously learned tasks.

Low-Rank Adaptation LoRA [19] is a widely adopted PEFT method used for fine-tuning various pre-trained models, particularly LMs. Specifically, let $W \in \mathbb{R}^{d_{out} \times d_{in}}$ represent a pre-trained weight in LMs, where d_{in} and d_{out} are the input and output dimensions, respectively. LoRA introduces an additional branch consisting of two matrices, $A \in \mathbb{R}^{d_{out} \times r}$ and $B \in \mathbb{R}^{r \times d_{in}}$, where $r \ll \min(d_{in}, d_{out})$. LoRA then modifies the forward propagation of this layer as $e = (W + AB)h$. Here, h and e denote the input and output, respectively. A is initialized to 0 , and B is initialized using a Gaussian distribution. During fine-tuning for downstream tasks, the pre-trained weight W remains frozen, and only the parameters A and B are fine-tuned.

3 Methodology

Our GainLoRA employs an expandable LoRA architecture, which is illustrated in Figure 1 (a). Specifically, before learning the t -th task ($1 \leq t \leq T$), GainLoRA first expands the LoRA architecture by introducing the t -th new branch with matrices $A_t \in \mathbb{R}^{d_{out} \times r}$ and $B_t \in \mathbb{R}^{r \times d_{in}}$. The new and old LoRA branches are then integrated as

$$W_t = W_{t-1} + a_t A_t B_t = \sum_{i=1}^t a_i A_i B_i, \quad (1)$$

where a_i is an integration coefficient that determines the contribution of the i -th LoRA branch to the input h . Note that W_{t-1} is a zero matrix when $t = 1$. As a result, the forward propagation in this layer is modified as

$$e = (W + W_t)h. \quad (2)$$

Finally, only the new LoRA branch (i.e. the t -th LoRA branch) is updated for the t -th new task, while all the old LoRA branches are frozen. After learning the t -th task, (2) is also used for inference across all test samples, thereby ensuring compatibility with the scenario where task identities are unavailable during inference.

Many existing CL methods based on LoRA [30, 46, 47, 57, 71] share a similar architecture to our method, as illustrated in Figure 1 (a). However, these methods fix all coefficients $\{a_i\}_{i=1}^t$ in (1) to 1, forcing the new and old LoRA branches to contribute equally to old tasks. As a result, the new LoRA branch introduces a change of $A_t B_t h$ to the output for inputs h associated with old tasks, potentially leading to forgetting. Although some methods attempt to mitigate this forgetting by imposing regularization [47] or orthogonality constraints [30] on the new LoRA branch, the fixed integration coefficients $\{a_i\}_{i=1}^t$ still limit their performance, as demonstrated by the experimental results presented in Section 4. Some method [71] does not force the new and old LoRA branches to contribute equally to old tasks but relies on replaying synthetic old samples to mitigate forgetting, making it unsuitable for the scenario considered in this work.

Different from existing methods, GainLoRA introduces an independent gating module $g_i(\cdot)$ for each task \mathcal{T}_i to generate the integration coefficients ($1 \leq i \leq T$). To mitigate the forgetting caused by the

new task, GainLoRA leverages the gating module to minimize the contribution from the new LoRA branch to the old tasks. The details will be introduced in the following subsections.

3.1 Architecture of Gating Modules

As illustrated in Figure 1 (b), given an input sample \mathbf{x} , the gating module $g_i(\cdot)$ generates the integration coefficient for the i -th LoRA branch, denoted as $a_i = g_i(\mathbf{x})$. The computation of $g_i(\cdot)$ is defined as

$$\mathbf{p}_0 = \text{Pool}(\text{Token}(\mathbf{x})), \mathbf{p}_l = \sigma(\mathbf{G}_{i,l}\mathbf{p}_{l-1}), l \in \{1, 2, \dots, L\}, g_i(\mathbf{x}) = f(\mathbf{G}_{i,L+1}\mathbf{p}_L). \quad (3)$$

Here, $\text{Token}(\cdot)$ represents the tokenizer used in LMs to extract token embeddings from the input \mathbf{x} . $\text{Pool}(\cdot)$ denotes an average pooling operation applied to the token embeddings to produce a fixed-size vector. $\sigma(\cdot)$ denotes the non-linear activation function. $\mathbf{G}_{i,l}$ denotes the weight matrix for the l -th layer of $g_i(\cdot)$ ($1 \leq l \leq L+1$). In the final layer, $\mathbf{G}_{i,L+1}$ is a vector that maps the input vector \mathbf{p}_{L+1} to a scalar. Following existing works with gating mechanisms [6, 17], the function $f(\cdot)$ is designed to map a scalar to a value within $[0, 1]$, that is, $f(\cdot) : \mathbb{R} \rightarrow [0, 1]$.

Note that the input to gating modules is the same as that of LMs, denoted as \mathbf{x} , which differs from the input to LoRA in a specific layer, denoted as \mathbf{h} . During the learning of the t -th new task, only the new gating module $g_t(\cdot)$ is updated, while all the old gating modules $\{g_i(\cdot)\}_{i=1}^{t-1}$ remain frozen.

3.2 Minimizing the Contribution from the new LoRA branch to Old Tasks

GainLoRA minimizes the contribution from the new LoRA branch to old tasks by making $a_t = g_t(\mathbf{x})$ as close to 0 as possible for any input \mathbf{x} from old tasks $\{\mathcal{T}_i\}_{i=1}^{t-1}$. However, since we focus on the scenario where no real or synthetic samples from old tasks are accessible, directly optimizing $g_t(\mathbf{x})$ to 0 is impractical. To overcome this challenge, GainLoRA imposes constraints on the new gating module $g_t(\cdot)$, implicitly guiding $g_t(\mathbf{x})$ to close to 0 and reduce the contribution of the new LoRA branch to old tasks.

In the following two subsections, we first describe the constraints imposed on the new gating module $g_t(\cdot)$ and explain how these constraints guide $g_t(\mathbf{x})$ close to 0 for any \mathbf{x} from the old tasks. Then, we detail the implementation of these constraints during training.

3.2.1 Constraints on New Gating Module

To formalize the constraints imposed on the new gating module $g_t(\cdot)$, we define the subspace spanned by the inputs to $\mathbf{G}_{t,l}$ ($1 \leq l \leq L+1$) from the previous $t-1$ tasks as:

$$\mathcal{M}_{t,l} = \text{span}\{\mathbf{p}_{l-1} \mid \mathbf{p}_{l-1} \text{ is defined in (3), } (\mathbf{x}, \mathbf{y}) \in \cup_{i=1}^{t-1} \mathcal{D}_i\}. \quad (4)$$

Note that subspaces $\{\mathcal{M}_{t,l}\}_{l=1}^{L+1}$ cannot be obtained directly due to the unavailability of samples from old tasks. However, by introducing additional constraints, $\{\mathcal{M}_{t,l}\}_{l=1}^{L+1}$ can be solved iteratively, which will be discussed in Section 3.2.2.

Initialization Constraints Before learning the t -th task, the following constraints are imposed on the initialization of the new gating module $g_t(\cdot)$:

$$\text{Init}(\mathbf{G}_{t,L+1}) \perp \mathcal{M}_{t,L+1}, f(0) = 0, \quad (5)$$

where $\text{Init}(\mathbf{G}_{t,L+1})$ denotes the initialization of $\mathbf{G}_{t,L+1}$. These constraints ensure that for any sample \mathbf{x} from the old tasks, the integration coefficient satisfies $a_t = g_t(\mathbf{x}) = f(\text{Init}(\mathbf{G}_{t,L+1})\mathbf{p}_L) = 0$, where \mathbf{p}_L is defined in (3). The second equality holds since $\mathbf{G}_{t,L+1} = \text{Init}(\mathbf{G}_{t,L+1})$ before learning the t -th new task. The third equality holds because $f(0) = 0$ and $\mathbf{p}_L \in \mathcal{M}_{t,L+1}$ for any \mathbf{x} from previous $t-1$ tasks.

Updating Constraints During the learning of the t -th task, the following constraints are imposed on the updates to the new gating module $g_t(\cdot)$:

$$\Delta \mathbf{G}_{t,l} \perp \mathcal{M}_{t,l} \quad \text{for } 1 \leq l \leq L+1, \quad (6)$$

where $\Delta \mathbf{G}_{t,l}$ denotes the update to $\mathbf{G}_{t,l}$. Based on existing studies [56, 28], the constraints in (6) ensure that $g_t(\mathbf{x})$ remains unchanged for inputs \mathbf{x} from the old tasks during the learning of the t -th task. Formally, the following proposition holds:

Proposition 3.1. *If the constraints in (6) are satisfied, subspaces $\{\mathcal{M}_{t,l}\}_{l=1}^{L+1}$ remain unchanged during the learning of the t -th task. Furthermore, for any input \mathbf{x} from the previous $t - 1$ tasks, $g_t(\mathbf{x})$ remains unchanged during the learning of the t -th task.*

The proof of this proposition is provided in Appendix A.3. Since the initialization constraints in (5) ensure $g_t(\mathbf{x}) = 0$ before learning the t -th new task, $g_t(\mathbf{x}) = 0$ is preserved throughout the learning process if the updating constraints in (6) are satisfied.

The fact that subspaces $\{\mathcal{M}_{t,l}\}_{l=1}^{L+1}$ remain unchanged, as stated in Proposition 3.1, is essential for implementing the orthogonal constraints in (6). Specifically, as will be detailed in Section 3.2.2, orthonormal bases for the subspaces $\{\mathcal{M}_{t,l}\}_{l=1}^{L+1}$ are learned to enforce the orthogonal constraints in (5) and (6). Since the subspaces $\{\mathcal{M}_{t,l}\}_{l=1}^{L+1}$ remain unchanged during the learning of the t -th task, their orthonormal bases also remain unchanged, allowing them to be pre-computed before learning the t -th task, thus facilitating the implementation of orthogonal constraints in (5) and (6) throughout the learning process.

3.2.2 Implementation of Constraints

There exist many functions $f(\cdot) : \mathbb{R} \rightarrow [0, 1]$ satisfying $f(0) = 0$. In this work, we define $f(\cdot)$ as

$$f(b) = |2 \cdot \text{sigmoid}(b) - 1|, \quad (7)$$

where $\text{sigmoid}(\cdot)$ denotes the sigmoid function. Other functions $f(\cdot) : \mathbb{R} \rightarrow [0, 1]$ that satisfy $f(0) = 0$ are also applicable, and experiments with different choices of $f(\cdot)$ are provided in Appendix C.4.1. Better model performance can be expected by designing more effective $f(\cdot)$, but this is not the focus of this paper.

Implementing the orthogonal constraints in (5) and (6) is challenging due to the lack of samples from previous $t - 1$ tasks to approximate the subspaces $\{\mathcal{M}_{t,l}\}_{l=1}^{L+1}$. To address this issue, we further impose the following constraints on the initialization of $\mathbf{G}_{t,l}$ ($1 \leq l \leq L$):

$$\text{Init}(\mathbf{G}_{t,l}) \leftarrow \mathbf{G}_{t-1,l}. \quad (8)$$

This strategy initializes the first L layers of $g_t(\cdot)$ using the corresponding layers from the previous gating module $g_{t-1}(\cdot)$. As a result, the first L layers of $g_t(\cdot)$ can be viewed as being initialized and starting their training at the beginning of the first task, continuing until the t -th task. Simultaneously, the first L layers in $g_i(\cdot)$ serve as checkpoints, preserving the state of $g_t(\cdot)$ after learning the i -th task ($1 \leq i \leq t$). At this time, we can use existing method gradient projection memory (GPM) [44] to iteratively learn a set of matrices $\{\mathbf{M}_{t,l}\}_{l=1}^{L+1}$, where the columns of $\mathbf{M}_{t,l}$ contribute to a set of orthonormal bases of subspace $\mathcal{M}_{t,l}$. Details of GPM are provided in Appendix A.1. Then, before learning the t -th task, the following operation can be performed on $\text{Init}(\mathbf{G}_{t,L+1})$:

$$\text{Init}(\mathbf{G}_{t,L+1}) \leftarrow \text{Init}(\mathbf{G}_{t,L+1}) - \mathbf{M}_{t,L+1} \mathbf{M}_{t,L+1}^T \text{Init}(\mathbf{G}_{t,L+1}). \quad (9)$$

According to existing works [28, 44, 56], $\text{Init}(\mathbf{G}_{t,L+1})$ satisfies the constraints in (5) after the operation in (9). Similarly, during the learning of the t -th task, the following operation can be performed on $\{\Delta \mathbf{G}_{t,l}\}_{l=1}^{L+1}$:

$$\Delta \mathbf{G}_{t,l} \leftarrow \Delta \mathbf{G}_{t,l} - \mathbf{M}_{t,l} \mathbf{M}_{t,l}^T \Delta \mathbf{G}_{t,l}. \quad (10)$$

After this, $\{\Delta \mathbf{G}_{t,l}\}_{l=1}^{L+1}$ satisfy the constraints in (6).

3.3 Updating the New LoRA Branch

Our GainLoRA aims to effectively integrate new and old LoRA branches while mitigating forgetting caused by the new LoRA branch on old tasks. Since GainLoRA does not impose specific update strategies for the new LoRA branch, it is inherently compatible with various existing CL methods that adopt similar LoRA architecture as our method and can update the new LoRA branch [30, 47, 57]. Since these existing methods fix all integration coefficients $\{a_i\}_{i=1}^t$ to 1, combining our method with these existing methods can enhance their performance, as demonstrated in Section 4.

Algorithm 1 GainLoRA for Continual Learning

Input: The data of different tasks $\{\mathcal{D}_t\}_{t=1}^T$.
Output: Learned LoRA parameters $\{(\mathbf{A}_i, \mathbf{B}_i)\}_{i=1}^T$ and gating modules $\{g_i(\cdot)\}_{i=1}^T$.
for t in $1 : T$ **do**
 Expand the t -th new LoRA branch with \mathbf{A}_t and \mathbf{B}_t ;
 Impose initialization constraints on the new gating module $g_t(\cdot)$ by (7), (8) and (9);
 Integrate new and old LoRA branches by (1);
 for $\mathcal{B}_t \subseteq \mathcal{D}_t$ **do**
 Compute the loss in (11) and the update of the new LoRA branch and the new gating module;
 Impose updating constraints on the update of the new gating module by (6);
 end for
end for

3.4 Whole Process of GainLoRA

Algorithm 1 outlines the whole process of our GainLoRA. Before learning the t -th new task \mathcal{T}_t , GainLoRA first expands the LoRA architecture by introducing the t -th new branch with matrices \mathbf{A}_t and \mathbf{B}_t . Simultaneously, a new gating module $g_t(\cdot)$ is initialized through the operations specified in (7), (9) and (8) to ensure that the initialization constraints in (5) are satisfied. The new and old LoRA branches are then integrated using (1), and the forward propagation is modified as (2).

During the learning of the t -th task \mathcal{T}_t with the corresponding dataset \mathcal{D}_t , our method follows existing methods [57, 71] and computes the loss for the new task through

$$\mathcal{L}_t = \frac{1}{|\mathcal{D}_t|} \sum_{(\mathbf{x}_t, \mathbf{y}_t) \in \mathcal{D}_t} \sum_{j=1}^{|\mathbf{y}_t|} \log [P(y_{t,j} | \mathbf{x}_t, y_{t,1}, \dots, y_{t,j-1})], \quad (11)$$

where $\mathbf{y}_t = [y_{t,1}, y_{t,2}, \dots, y_{t,|\mathbf{y}_t|}]$. Each time, GainLoRA samples a mini-batch \mathcal{B}_t to minimize the loss in (11) by updating the new LoRA branch and the new gating module $g_t(\cdot)$. During this process, the projections defined in (10) are applied to the parameters of $g_t(\cdot)$, ensuring that the update constraints in (6) are satisfied.

GainLoRA introduces a new gating module for each new task, which incurs additional parameters and computational cost when combined with other methods. Section 4 will demonstrate that the trainable parameters added by GainLoRA are limited, making the number of trainable parameters in GainLoRA comparable to other methods. Additionally, Appendix C.1 and C.2 will demonstrate that the computational cost introduced by GainLoRA is minimal compared to the original LMs.

4 Experiments

4.1 Experimental Settings

Datasets Following existing CL methods [42, 57, 71], we evaluate different methods on SuperNI [60] and Long Sequence [42] benchmarks. SuperNI benchmark includes various types of NLP tasks, including dialogue generation, information extraction, question answering, summarization, and sentiment analysis. Following the protocols of existing method [71], three tasks are selected from each type, resulting in 15 tasks. These tasks are arranged into two different task sequences with different orders, referred to as Order 1 and Order 2. Long Sequence benchmark consists of 15 diverse classification tasks, which are similarly arranged into two task sequences with different orders, referred to as Order 3 and Order 4. More details about the benchmarks and task sequences are provided in Appendix B.

Evaluation Metric We use $A_{j,i}$ to denote the model’s performance on the i -th task once the model learns the j -th task. Specifically, $A_{j,i}$ represents accuracy for classification tasks and Rouge-L [31] for other types of tasks. Following traditional CL works [4, 5], we employ average performance (AP) and forgetting (FT) to evaluate the model’s performance. The formulas for these two metrics are provided in Appendix B.1.

Baselines We compare our method with state-of-the-art CL methods, including LFPT5 [39], EPI [61], MIGU [10], EWC [22], TASL [13], KIFLoRA [12], IncLoRA [57], C-LoRA [47], O-LoRA [57],

Table 1: Results on different task sequences with T5-large model. Results of methods with * are copied from existing paper [71].

Method	Order 1		Order 2		Order 3		Order 4	
	AP \uparrow	FT \downarrow	AP \uparrow	FT \downarrow	AP \uparrow	FT \downarrow	AP \uparrow	FT \downarrow
LFPT5* [39]	39.03	10.87	29.70	20.72	66.62	14.57	67.40	13.20
EPI* [61]	-	-	-	-	75.19	0.77	75.10	2.44
MIGU+FT [10]	-	-	-	-	71.30	11.39	69.05	14.06
EWC [22]	15.32	26.78	18.19	30.28	43.24	23.66	46.25	32.90
TaSL [13]	27.51	18.53	28.05	17.39	71.37	6.20	73.11	6.52
KIFLoRA [12]	28.33	16.44	30.31	16.27	72.19	3.10	73.72	4.75
SeqLoRA	7.30	47.60	7.03	47.97	49.46	27.60	33.81	45.53
IncLoRA [57]	12.33	41.93	16.65	36.56	61.19	13.63	62.46	15.92
C-LoRA [47]	22.69	24.25	32.81	11.60	66.83	8.64	61.86	14.18
O-LoRA [57]	26.37	19.15	32.83	11.99	70.98	3.69	71.21	4.03
GainLoRA (O-LoRA)	47.84	2.26	46.84	2.91	73.37	3.02	76.01	2.49
InfLoRA [30]	39.78	7.64	39.57	8.93	75.15	4.19	75.79	3.47
GainLoRA (InfLoRA)	46.21	2.40	46.44	2.61	78.01	0.77	77.54	1.25

and InfLoRA [30]. Additionally, we introduce a simple baseline called SeqLoRA, which does not expand new LoRA branches but sequentially updates old LoRA parameters for new tasks and lacks mechanism to mitigate forgetting. Note that many CL methods based on pre-trained models in CV focus on classification tasks, relying either on carefully designed classifiers [36, 67, 70] or the [CLS] token in ViT [23, 48, 53, 54, 59, 62, 63]. In contrast, we follow existing works in NLP [57, 71] and adopt next-token prediction to handle both classification and generation tasks, where models [40, 51] lack a [CLS] token. Consequently, these CV methods are incompatible with our setting and cannot be directly compared. For completeness, we adapt some of them to our setup and report results in Appendix C.9.

Implementation Details Following existing CL works [37, 57, 64], all methods are implemented with instruction tuning [37] and optimized using AdamW [33]. To ensure fair comparisons, for all the methods based on LoRA, we follow existing CL methods [19, 57, 71] by incorporating the LoRA architecture into the query and value components of the multi-head attention mechanism in each Transformer block. We use T5 [40] and Llama-2 [51] as the base architectures, aligning with the existing CL methods for LMs [57, 71]. Each experiment is repeated three times with different seeds, and the average result is reported. More details, such as the learning rate, batch size, and architecture of the gating modules in GainLoRA, are provided in Appendix B.3 and Appendix B.4.

4.2 Experimental Results

Compare with Existing Methods We first follow existing works [10, 71] and evaluate different CL methods using T5-Large. Since our method does not impose specific update strategies for the new LoRA branch, we adopt the same update strategies as the two state-of-the-art methods, O-LoRA [57] and InfLoRA [30]. Note that these two methods leverage LoRA architecture similar to our method but fix all integration coefficients $\{a_i\}_{i=1}^T$ to 1. Details of these two methods are provided in Appendix A.2. We use GainLoRA (O-LoRA) and GainLoRA (InfLoRA) to respectively denote our methods adopting O-LoRA and InfLoRA to update the new LoRA branch. GainLoRA is also compatible with other methods that leverage expandable LoRA architecture shown in Figure 1 (a), and we give some results in Appendix C.6.

The results are shown in Table 1. As we can see, our methods GainLoRA (O-LoRA) and GainLoRA (InfLoRA) outperform O-LoRA and InfLoRA in both AP and FT, respectively. This improvement demonstrates that fixing all coefficients $\{a_i\}_{i=1}^T$ to 1 leads to forgetting on old tasks, thereby limiting the performance of O-LoRA and InfLoRA. By effectively mitigating this forgetting, GainLoRA (O-LoRA) and GainLoRA (InfLoRA) achieve superior performance. Furthermore, our methods consistently achieve the best performance across all task sequences.

Figure 2 illustrates the variation in the average performance across all learned tasks for different methods throughout the CL process. As shown, GainLoRA consistently outperforms the performance of O-LoRA and InfLoRA throughout the whole training process.

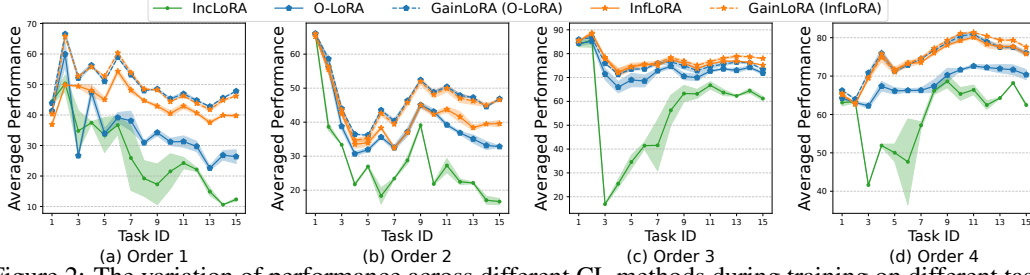


Figure 2: The variation of performance across different CL methods during training on different task sequences.

Table 2: The overall results on different task sequences with T5-XL model.

Method	Order 1		Order 2		Order 3		Order 4	
	AP \uparrow	FT \downarrow	AP \uparrow	FT \downarrow	AP \uparrow	FT \downarrow	AP \uparrow	FT \downarrow
O-LoRA [57]	36.50	11.42	40.64	6.37	73.77	2.70	76.19	3.56
GainLoRA (O-LoRA)	50.10	3.21	49.86	3.04	78.41	2.59	77.21	3.30
InfLoRA [30]	45.61	5.60	45.85	5.10	80.22	2.09	79.43	1.71
GainLoRA (InfLoRA)	50.06	1.86	50.26	2.64	81.22	0.58	80.30	0.75

Table 3: The overall results on different task sequences with Llama-2-7B and Llama-2-13B.

Method	Llama-2-7B				Llama-2-13B			
	Order 1		Order 2		Order 1		Order 2	
	AP \uparrow	FT \downarrow	AP \uparrow	FT \downarrow	AP \uparrow	FT \downarrow	AP \uparrow	FT \downarrow
O-LoRA [57]	39.37	15.84	37.55	20.23	43.92	14.15	40.05	19.53
GainLoRA (O-LoRA)	51.10	4.96	51.14	5.57	52.47	4.78	51.68	5.86
InfLoRA [30]	42.93	11.23	39.94	15.00	43.64	14.85	45.74	10.61
GainLoRA (InfLoRA)	51.27	2.84	50.17	4.71	53.64	2.87	52.46	4.90

Scaling to Larger Model Architectures To evaluate the effectiveness of our method on larger model architectures, we scale different LoRA-based CL methods to larger models, including T5-XL, Llama-2-7B, and Llama-2-13B. Table 2 and Table 3 present the results of different methods. As shown, across models of varying sizes, GainLoRA (O-LoRA) and GainLoRA (InfLoRA) consistently outperform O-LoRA and InfLoRA in terms of AP and FT, respectively. This demonstrates that GainLoRA effectively mitigates forgetting in the new LoRA branch across different model architectures.

Trainable Parameters We compare the number of trainable parameters across different methods for training on different task sequences. The results are shown in Figure 3 (a) and Figure 3 (b), and the detailed computation of trainable parameters is provided in Appendix B.5. As shown, GainLoRA (O-LoRA) and GainLoRA (InfLoRA) have more trainable parameters than O-LoRA and InfLoRA, respectively. This increase arises from the introduction of the trainable gating module in GainLoRA. However, the additional trainable parameters introduced by GainLoRA are much fewer than those in LoRA. Therefore, the total number of trainable parameters in GainLoRA (O-LoRA) and GainLoRA (InfLoRA) are comparable to that of O-LoRA and InfLoRA, respectively.

Distribution of Outputs in New Gating Module To demonstrate that our GainLoRA effectively minimizes the contribution from the new LoRA branches to old tasks, we analyze the output distributions of the new gating modules. Specifically, after training on the final task (i.e., the 15-th task) in the task sequences, the 15-th task corresponds to the new task, and its associated gating module $g_{15}(\cdot)$ serves as the new gating module.

We obtain the outputs of the new gating module $g_{15}(\cdot)$ on the samples from old and new tasks, respectively. Then, we analyze their distributions in Figure 3 (c) and Figure 3 (d). As shown, the outputs of $g_{15}(\cdot)$ for the samples from old tasks are concentrated around 0, effectively minimizing the contribution from the new LoRA branch to old tasks. Furthermore, GainLoRA does not constrain the outputs of $g_{15}(\cdot)$ for the samples from the new task. As a result, the outputs of $g_{15}(\cdot)$ for the samples from the new task are distributed near 1, enabling the model to effectively learn the new task.

Ablation Study To verify the necessity of both the initialization and updating constraints introduced in Section 3.2.1, we define several variants of GainLoRA. The first variant, referred to as “No

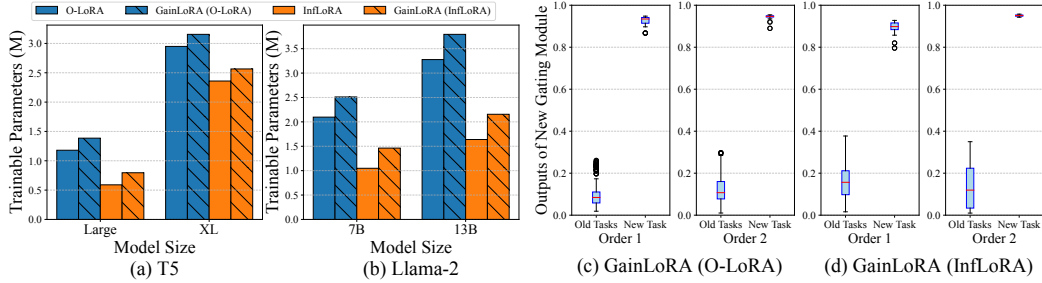


Figure 3: (a) and (b) show the number of trainable parameters in different CL methods with different model backbones on task sequences Order 1 and Order 2. (c) and (d) show outputs of new gating module in our GainLoRA on different task sequences with T5-Large.

Table 4: Ablation study of GainLoRA with T5-Large and Llama-2-7B.

Method	T5-Large				Llama-2-7B			
	Order 1		Order 2		Order 1		Order 2	
	AP↑	FT↓	AP↑	FT↓	AP↑	FT↓	AP↑	FT↓
GainLoRA (O-LoRA)	47.84	2.26	46.84	2.91	51.10	4.96	51.14	5.57
No Initialization Constraints	35.30	17.19	39.82	12.90	44.02	11.71	42.89	14.77
No Updating Constraints	23.01	30.32	24.96	28.14	33.74	23.06	34.71	22.36
No Constraints	26.32	26.00	30.63	22.37	34.48	23.46	36.87	21.24
GainLoRA (InfLoRA)	46.21	2.40	46.44	2.61	51.27	2.84	50.17	4.71
No Initialization Constraints	45.38	3.40	43.05	5.15	50.48	3.48	48.17	6.45
No Updating Constraints	37.69	10.94	38.85	9.31	48.52	5.68	47.85	7.00
No Constraints	36.75	12.18	41.00	6.66	49.10	6.07	45.77	8.70

Initialization Constraints”, removes the initialization constraints defined in (5). Specifically, it replaces $f(\cdot)$ defined in (7) with function $\text{sigmoid}(\cdot)$ and eliminates the operation in (9) while keeping all other components unchanged. The second variant, referred to as “No Updating Constraints”, removes the updating constraints defined in (6) by eliminating the operations in (10) while preserving all other components of GainLoRA. The third variant, referred to as “No Constraints”, follows “No Initialization Constraints” and “No Updating Constraints” to remove both the initialization and updating constraints. Table 4 presents the experimental results of these variants. As shown, none of these variants perform as well as our GainLoRA, indicating the critical role of both the initialization constraints and updating constraints in our GainLoRA.

5 Conclusion

In this work, we propose a new method, called GainLoRA, for CL of language models. GainLoRA expands a new LoRA branch for each new task and introduces gating modules to integrate the new and old LoRA branches. Furthermore, GainLoRA leverages the new gating module to minimize the contribution of the new LoRA branch to old tasks, effectively mitigating forgetting and improving the model’s overall performance. Experimental results on CL benchmarks demonstrate that GainLoRA outperforms existing state-of-the-art methods.

Limitations Similar to many CL methods for LMs [13, 57], our method imposes constraints on the model to mitigate forgetting. Specifically, we adopt orthogonal constraints, whereas other methods employ alternative strategies such as orthogonal [57] or mask-based constraints [13]. While effective, these constraints may accumulate with increasing tasks, potentially hindering the learning of new tasks. Furthermore, consistent with existing works [22, 30, 57], our method primarily targets at catastrophic forgetting, and further investigation is needed to assess its effect on forward and backward knowledge transfer.

6 Broader Impacts

Continual learning (CL) offers a promising direction for improving the efficiency and scalability of language models, particularly in settings with continuously arriving tasks. By enabling incremental updates without retraining from scratch, it significantly reduces computational overhead and resource demands. However, CL often introduces additional components (e.g. memory or gating mechanisms), increasing complexity and requiring effort for maintenance or deployment.

A More Details of Methods

A.1 Gradient Projection Memory

We initialize the first L layers of $g_t(\cdot)$ using the corresponding layers from the previous gating module $g_{t-1}(\cdot)$. Therefore, the first L layers of $g_t(\cdot)$ can be viewed as being initialized at the beginning of the first task and continue their training until the t -th task. Additionally, the first L layers in $g_i(\cdot)$ serve as checkpoints, preserving the state of $g_t(\cdot)$ after learning the i -th task ($1 \leq i \leq t$). At this time, existing method gradient projection memory (GPM) [44] can be used to learn matrices $\{\mathbf{M}_{t,l}\}_{l=1}^{L+1}$, where the columns of $\mathbf{M}_{t,l}$ approximate the orthonormal bases of the subspace $\mathcal{M}_{t,l}$. Specifically, when $t = 1$, since there is no old task, $\mathcal{M}_{1,l}$ is a null space and $\mathbf{M}_{1,l}$ is a zero matrix. After learning the t -th new task, GPM expands $\mathcal{M}_{t,l}$ to $\mathcal{M}_{t+1,l}$ by first computing the input matrix $\mathbf{H}_{t,l}$ where each column of $\mathbf{H}_{t,l}$ represents an input to the l -th layer. Then, the component of $\mathbf{H}_{t,l}$ already in $\mathcal{M}_{t,l}$ is removed by

$$\widehat{\mathbf{H}}_{t,l} = \mathbf{H}_{t,l} - \mathbf{M}_{t,l}(\mathbf{M}_{t,l})^T \mathbf{H}_{t,l}. \quad (12)$$

Next, singular value decomposition (SVD) is performed on $\widehat{\mathbf{H}}_{t,l} \widehat{\mathbf{H}}_{t,l}^T$, which is decomposed as $\widehat{\mathbf{U}}_{t,l} \widehat{\Sigma}_{t,l} \widehat{\mathbf{U}}_{t,l}^T$. Then, u new orthonormal bases $\mathbf{u}_1, \dots, \mathbf{u}_u$ are chosen from the columns of $\widehat{\mathbf{U}}_{t,l}$, where u is the minimum number satisfying the following criteria for a given threshold ϵ_{th} :

$$\|(\widehat{\mathbf{H}}_{t,l})_u\|_F^2 + \|\mathbf{M}_{t,l}(\mathbf{M}_{t,l})^T \mathbf{H}_{t,l}\|_F^2 \geq \epsilon_{th} \|\mathbf{H}_{t,l}\|_F^2. \quad (13)$$

Here, $(\widehat{\mathbf{H}}_{t,l})_u$ denotes the components of $\widehat{\mathbf{H}}_{t,l}$ corresponding to the top- u singular values. Then, the orthonormal bases of subspace $\mathcal{M}_{t+1,l}$ are obtained by augmenting the orthonormal bases of subspace $\mathcal{M}_{t,l}$ with the new orthogonal vectors $\mathbf{u}_1, \dots, \mathbf{u}_u$, resulting in $\mathbf{M}_{t+1,l} = [\mathbf{M}_{t,l}, \mathbf{u}_1, \dots, \mathbf{u}_u]$.

A.2 More Details of O-LoRA and InfLoRA

O-LoRA O-LoRA [57] ensures that the new LoRA branch remains orthogonal to all the old LoRA branches. Specifically, during the learning of the t -th new task with the t -th LoRA branch $(\mathbf{A}_t, \mathbf{B}_t)$, O-LoRA computes the inner product between the new and old LoRA branches as

$$\mathbf{O}_{i,t} = \mathbf{B}_i^T \mathbf{B}_t \quad \text{for } 1 \leq i \leq t-1 \quad (14)$$

Then, the loss function of O-LoRA is defined as

$$\frac{1}{|\mathcal{D}_t|} \sum_{(\mathbf{x}_t, \mathbf{y}_t) \in \mathcal{D}_t} \sum_{j=1}^{|\mathbf{y}_t|} \log [P(y_{t,j} | \mathbf{x}_t, y_{t,1}, \dots, y_{t,j-1})] + \lambda \sum_{i=1}^{t-1} \sum_{j,k} \|\mathbf{O}_{i,t}[j, k]\|_2^2 \quad (15)$$

For further details on O-LoRA, we refer readers to the original paper [57].

InfLoRA InfLoRA [30] ensures orthogonality between the new LoRA branch and the gradients of old tasks. Specifically, it shows that only fine-tuning the down-projection matrix \mathbf{A}_t in the new LoRA branch is equivalent to directly fine-tuning the pre-trained weights within a subspace spanned by the rows of \mathbf{B}_t . Therefore, before learning the t -th task, InfLoRA designs \mathbf{B}_t to be orthogonal to the gradients of the old tasks. During the learning of the t -th task, InfLoRA only tunes \mathbf{A}_t in the new LoRA branch while freezing \mathbf{B}_t and all the old LoRA branches. For further details on InfLoRA, we refer readers to the original paper [30].

A.3 Proof of Proposition 3.1

Proposition A.1. *If the constraints in (6) are satisfied, subspaces $\{\mathcal{M}_{t,l}\}_{l=1}^{L+1}$ remain unchanged during the learning of the t -th task. Furthermore, for any input \mathbf{x} from the previous $t - 1$ tasks, $g_t(\mathbf{x})$ remains unchanged during the learning of the t -th task.*

Proof. For any \mathbf{x} from previous $t - 1$ tasks, we rewrite $g_t(\mathbf{x})$ as

$$\begin{aligned} g_t(\mathbf{x}) &= f(\mathbf{G}_{t,L+1}\mathbf{p}_L), \\ \mathbf{p}_l &= \sigma(\mathbf{G}_{t,l}\mathbf{p}_{l-1}), \quad l \in \{1, 2, \dots, L\}, \\ \mathbf{p}_0 &= \text{Pool}(\text{Token}(\mathbf{x})). \end{aligned} \quad (16)$$

Since $\mathbf{p}_0 = \text{Pool}(\text{Token}(\mathbf{x}))$ is unrelated to the parameters of the new gating module $g_t(\cdot)$, \mathbf{p}_0 does not change with the update of $g_t(\cdot)$. Since $\mathcal{M}_{t,1}$ is spanned by \mathbf{p}_0 , $\mathcal{M}_{t,1}$ remains unchanged during the learning of the t -th task.

Suppose that we have proven that \mathbf{p}_{l-1} does not change with the update of the new gating module $g_t(\cdot)$ ($1 \leq l \leq L$). Since $\mathcal{M}_{t,l}$ is spanned by \mathbf{p}_{l-1} , $\mathcal{M}_{t,l}$ remains unchanged during the learning of the t -th task. At this point, \mathbf{p}_l can be expressed as

$$\mathbf{p}_l = \sigma((\text{Init}(\mathbf{G}_{t,l}) + \Delta\mathbf{G}_{t,l})\mathbf{p}_{l-1}) = \sigma(\text{Init}(\mathbf{G}_{t,l})\mathbf{p}_{l-1}). \quad (17)$$

Here, the second equality holds since $\mathbf{p}_{l-1} \in \mathcal{M}_{t,l}$ and $\Delta\mathbf{G}_{t,l} \perp \mathcal{M}_{t,l}$. Therefore, \mathbf{p}_l does not change with the update of the new gating module $g_t(\cdot)$ ($1 \leq l \leq L$). Since $\mathcal{M}_{t,L+1}$ is spanned by \mathbf{p}_L , $\mathcal{M}_{t,L+1}$ remains unchanged during the learning of the t -th task.

Furthermore, during the learning of the t -th task, $g_t(\mathbf{x})$ can be expressed as

$$g_t(\mathbf{x}) = f((\text{Init}(\mathbf{G}_{t,L+1}) + \Delta\mathbf{G}_{t,L+1})\mathbf{p}_L) = f(\text{Init}(\mathbf{G}_{t,L+1})\mathbf{p}_L). \quad (18)$$

Here, the second equality holds since $\mathbf{p}_L \in \mathcal{M}_{t,L+1}$ and $\Delta\mathbf{G}_{t,L+1} \perp \mathcal{M}_{t,L+1}$. \square

B More Details of Experimental Settings

B.1 Evaluation Metrics

We use $A_{j,i}$ to denote the model’s performance on the i -th task once the model learns the j -th task. Specifically, $A_{j,i}$ represents accuracy for classification tasks and Rouge-L [31] for other types of tasks. Following traditional CL works [4, 5], we employ average performance (AP) and forgetting (FT) to evaluate the model’s performance. The formulas for these two metrics are defined as

$$\text{AP} = \frac{1}{T} \sum_{i=1}^T A_{T,i}, \quad \text{FT} = \frac{1}{T-1} \sum_{i=1}^{T-1} (\max_{l \in \{1, 2, \dots, T-1\}} A_{l,i} - A_{T,i}), \quad (19)$$

where T denotes the total number of tasks in the task sequence. AP evaluates the model’s final performance, and FT quantifies the forgetting.

B.2 More Details of Datasets

Table 5 and Table 6 show the details of Long Sequence Benchmark and SuperNI Benchmark, respectively. Long Sequence Benchmark consists of 15 classification tasks while SuperNI Benchmark consists of various NLP tasks, including dialogue generation, information extraction, question answering, summarization, and sentiment analysis.

The task sequences are constructed using Long Sequence Benchmark and SuperNI Benchmark. The details of different task sequences are presented in Table 7.

B.3 More Implementation Details

Following existing CL works [37, 57, 64], all methods are implemented using instruction tuning [37]. Experiments are conducted on 5 NVIDIA RTX A6000 GPUs with AdamW [33] as the optimizer. The type of CPU is Intel(R) Xeon(R) Gold 6240R CPU @ 2.40GHz. For T5-Large and T5-XL,

Table 5: Details of different tasks in Long Benchmark.

Dataset name	Category	Domain	Task Type	Metric
Yelp	CL Benchmark	sentiment analysis	Yelp reviews	Accuracy
Amazon	CL Benchmark	sentiment analysis	Amazon reviews	Accuracy
DBpedia	CL Benchmark	topic classification	Wikipedia	Accuracy
Yahoo	CL Benchmark	topic classification	Yahoo Q&A	Accuracy
AG News	CL Benchmark	topic classification	news	Accuracy
MNLI	GLUE	natural language inference	various	Accuracy
QQP	GLUE	paraphrase detection	Quora	Accuracy
RTE	GLUE	natural language inference	news, Wikipedia	Accuracy
SST-2	GLUE	sentiment analysis	movie reviews	Accuracy
WiC	SuperGLUE	word sense disambiguation	lexical databases	Accuracy
CB	SuperGLUE	natural language inference	various	Accuracy
COPA	SuperGLUE	question and answering	blogs, encyclopedia	Accuracy
BoolQA	SuperGLUE	boolean question and answering	Wikipedia	Accuracy
MultiRC	SuperGLUE	question and answering	various	Accuracy
IMDB	SuperGLUE	sentiment analysis	movie reviews	Accuracy

Table 6: Details of different tasks in SuperNI Benchmark.

Dataset name	Task Type	Metric
Task639_multi_woz_user_utterance_generation	summarization	Rouge-L
Task1590_diplomacy_text_generation	summarization	Rouge-L
Task1729_personachat_generate_next	summarization	Rouge-L
Task181_outcome_extraction	information extraction	Rouge-L
Task748_glucose_reverse_cause_event_detection	information extraction	Rouge-L
Task1510_evaluation_relation_extraction	information extraction	Rouge-L
Task002_quoref_answer_generation	dialogue generation	Rouge-L
Task073_commonsenseqa_answer_generation	dialogue generation	Rouge-L
Task591_sciq_answer_generation	dialogue generation	Rouge-L
Task511_reddit_tifu_long_text_summarization	question answering	Rouge-L
Task1290_xsum_summarization	question answering	Rouge-L
Task1572_samsum_summary	question answering	Rouge-L
Task363_sst2_polarity_classification	sentiment analysis	Accuracy
Task875_emotion_classification	sentiment analysis	Accuracy
Task1687_sentiment140_classification	sentiment analysis	Accuracy

their relatively smaller model sizes allow experiments to be performed on a single A6000 GPU with gradient accumulation. For Llama-2-7B and Llama-2-13B, data parallelism with DeepSpeed ZeRO-2 [41] is prioritized across multiple A6000 GPUs. FlashAttention-2 [8] is employed to reduce memory usage during training, ensuring sufficient GPU memory to enable DeepSpeed ZeRO-2 whenever possible. However, if the sequence lengths of certain tasks are too long to enable DeepSpeed ZeRO-2 even with FlashAttention-2, DeepSpeed ZeRO-3 is utilized to handle these tasks.

To ensure fair comparisons, for all the methods based on LoRA, we follow existing CL methods [19, 57, 71] by integrating the LoRA architecture into the query and value components of the multi-head attention mechanism in each Transformer block. Following existing works [57, 71], for all the methods based on LoRA, the rank of a single LoRA branch is set to 4 for Order 1 and Order 2, and 8 for Order 3 and Order 4. We also vary the rank in LoRA branches and show the results in Appendix C.5.

Table 7: The order of different task sequences for experiments.

Benchmark	Order	Task Sequence
SuperNI Benchmark	1	task1572 → task363 → task1290 → task181 → task002 → task1510 → task639 → task1729 → task073 → task1590 → task748 → task511 → task591 → task1687 → task875
	2	task748 → task073 → task1590 → task639 → task1572 → task1687 → task591 → task363 → task1510 → task1729 → task181 → task511 → task002 → task1290 → task875
CL Benchmark	3	MNLI → CB → WiC → COPA → QQP → BoolQA → RTE → IMDB → Yelp → Amazon → SST-2 → DBpedia → AG News → MultiRC → Yahoo
	4	Yelp → Amazon → MNLI → CB → COPA → QQP → RTE → IMDB → SST-2 → DBpedia → AG News → Yahoo → MultiRC → BoolQA → WiC

For our methods, the global batch size is set to 32 across all model backbones. The learning rate is set to $3e-4$ for T5 backbones and $5e-5$ for Llama backbones. Each task is trained for 100 epochs with T5 backbones and 50 epochs with Llama backbones. For baselines, we follow their official implementations to set the hyperparameters, making the comparison as fair as possible. If this does not achieve the expected performance, we perform a hyperparameter search for the learning rate and batch size.

B.4 More Details about the Architecture of the Gating Module

The architecture of the gating module $g_i(\cdot)$ can be represented as

$$\begin{aligned}
g_i(\mathbf{x}) &= f(\mathbf{G}_{i,L+1}\mathbf{p}_L), \\
\mathbf{p}_l &= \sigma(\mathbf{G}_{i,l}\mathbf{p}_{l-1}), \quad l \in \{1, 2, \dots, L\}, \\
\mathbf{p}_0 &= \text{Pool}(\text{Token}(\mathbf{x})).
\end{aligned} \tag{20}$$

Non-linear activation function $\sigma(\cdot)$ is set to SiLU [11]. For all experiments, unless otherwise stated, L is set to 2. In other words, the gating module $g_i(\cdot)$ has three layers. For T5-Large and T5-XL, the parameters in the i -th gating module $g_i(\cdot)$ are $\mathbf{G}_{i,1} \in \mathbb{R}^{100 \times d}$, $\mathbf{G}_{i,2} \in \mathbb{R}^{d \times 100}$ and $\mathbf{G}_{i,3} \in \mathbb{R}^{1 \times d}$. For Llama-2-7B and Llama-2-13B, the parameters in the i -th gating module $g_i(\cdot)$ are $\mathbf{G}_{i,1} \in \mathbb{R}^{50 \times d}$, $\mathbf{G}_{i,2} \in \mathbb{R}^{d \times 50}$ and $\mathbf{G}_{i,3} \in \mathbb{R}^{1 \times d}$. Here, d denotes the dimension of the embeddings. For different models, d is 1024 for T5-Large and T5-XL, 4096 for Llama-2-7B, and 5120 for Llama-2-13B.

Additionally, we investigate the influence of the architecture of the gating module on the performance of our method. Results are provided in Appendix C.4.

B.5 Computation of Trainable Parameters

To ensure fair comparisons, we set the same rank for each LoRA branch across all CL methods based on the expandable LoRA architectures shown in Figure 1 (a). Additionally, for all the methods based on LoRA, the LoRA modules are incorporated into the query and value components of the multi-head attention mechanism within each Transformer block.

B.5.1 Computation of Trainable Parameters in T5-Large

In T5-Large, the projection weights for the query and value components have shapes $\mathbf{W}_q, \mathbf{W}_v \in \mathbb{R}^{1024 \times 1024}$. The model consists of 24 self-attention modules in the encoder, 24 self-attention modules in the decoder, and 24 cross-attention modules in the decoder, resulting in a total of $(24 + 24 + 24) * 2 = 144$ pre-trained weights that incorporate the LoRA architecture.

During the learning of the t -th new task, O-LoRA updates the parameters $\mathbf{A}_t \in \mathbb{R}^{1024 \times r}$ and $\mathbf{B}_t \in \mathbb{R}^{r \times 1024}$, resulting in $1024 * r * 144 + r * 1024 * 144 = 294912r$ trainable parameters. When $r = 4$, the number of trainable parameters in O-LoRA is $294912 * 4 = 1179648 = 1.18\text{M}$. InfLoRA only

updates the parameters $\mathbf{A}_t \in \mathbb{R}^{1024 \times r}$, resulting in $1024 * r * 144 = 147456r$ trainable parameters. When $r = 4$, the number of trainable parameters in InfLoRA is $147456r = 589824 = 0.59\text{M}$.

GainLoRA introduces an additional new gating module $g_t(\cdot)$ with parameters $\mathbf{G}_{t,1} \in \mathbb{R}^{100 \times 1024}$, $\mathbf{G}_{t,2} \in \mathbb{R}^{1024 \times 100}$ and $\mathbf{G}_{t,3} \in \mathbb{R}^{1 \times 1024}$. Therefore, the number of trainable parameters in GainLoRA (O-LoRA) is $1179648 + 1024 * 100 + 1024 * 100 + 1024 = 1385472 = 1.39\text{M}$. The number of trainable parameters in GainLoRA (InfLoRA) is $589824 + 1024 * 100 + 1024 * 100 + 1024 = 795648 = 0.80\text{M}$.

B.5.2 Computation of Trainable Parameters in T5-XL

In T5-XL, the projection weights for the query and value components have shapes $\mathbf{W}_q, \mathbf{W}_v \in \mathbb{R}^{4096 \times 1024}$. The model architecture is similar to T5-Large, with 144 pre-trained weights incorporating LoRA.

During the learning of the t -th new task, O-LoRA updates the parameters $\mathbf{A}_t \in \mathbb{R}^{4096 \times r}$ and $\mathbf{B}_t \in \mathbb{R}^{r \times 1024}$, resulting in $4096 * r * 144 + r * 1024 * 144 = 737280r$ trainable parameters. When $r = 4$, O-LoRA has $737280 * 4 = 2949120 = 2.95\text{M}$ trainable parameters. InfLoRA only updates $\mathbf{A}_t \in \mathbb{R}^{4096 \times r}$, resulting in $4096 * r * 144 = 589824r$ trainable parameters. When $r = 4$, InfLoRA has $589824 * 4 = 2359296 = 2.36\text{M}$ trainable parameters.

GainLoRA introduces the same new gating module $g_t(\cdot)$ as in T5-Large, with parameters $\mathbf{G}_{t,1} \in \mathbb{R}^{100 \times 1024}$, $\mathbf{G}_{t,2} \in \mathbb{R}^{1024 \times 100}$ and $\mathbf{G}_{t,3} \in \mathbb{R}^{1 \times 1024}$. Thus, the total number of trainable parameters for GainLoRA (O-LoRA) is $2949120 + 1024 * 100 + 1024 * 100 + 1024 = 3154944 = 3.15\text{M}$. The total number of trainable parameters in GainLoRA (InfLoRA) is $2359296 + 1024 * 100 + 1024 * 100 + 1024 = 2565120 = 2.57\text{M}$.

B.5.3 Computation of Trainable Parameters in Llama-2-7B

In Llama-2-7B, the projection weights for the query and value components have shapes $\mathbf{W}_q, \mathbf{W}_v \in \mathbb{R}^{4096 \times 4096}$. The model contains 32 self-attention modules, resulting in $32 * 2 = 64$ pre-trained weights that incorporate the LoRA architecture.

During the learning of the t -th new task, O-LoRA updates the parameters $\mathbf{A}_t \in \mathbb{R}^{4096 \times r}$ and $\mathbf{B}_t \in \mathbb{R}^{r \times 4096}$, resulting in $4096 * r * 64 + r * 4096 * 64 = 524288r$ trainable parameters. When $r = 4$, the number of trainable parameters in O-LoRA is $524288 * 4 = 2097152 = 2.10\text{M}$. InfLoRA only updates the parameters $\mathbf{A}_t \in \mathbb{R}^{4096 \times r}$, resulting in $4096 * r * 64 = 262144r$ trainable parameters. When $r = 4$, the number of trainable parameters in InfLoRA is $262144 * 4 = 1048576 = 1.05\text{M}$.

GainLoRA introduces a new gating module $g_t(\cdot)$ with parameters $\mathbf{G}_{t,1} \in \mathbb{R}^{50 \times 4096}$, $\mathbf{G}_{t,2} \in \mathbb{R}^{4096 \times 50}$ and $\mathbf{G}_{t,3} \in \mathbb{R}^{1 \times 4096}$. Therefore, the number of trainable parameters in GainLoRA (O-LoRA) is $2097152 + 4096 * 50 + 4096 * 50 + 4096 = 2510848 = 2.51\text{M}$. The number of trainable parameters in GainLoRA (InfLoRA) is $1048576 + 4096 * 50 + 4096 * 50 + 4096 = 1462272 = 1.46\text{M}$.

B.5.4 Computation of Trainable Parameters in Llama-2-13B

In Llama-2-13B, the projection weights for the query and value components have shapes $\mathbf{W}_q, \mathbf{W}_v \in \mathbb{R}^{5120 \times 5120}$. The model contains 40 self-attention modules, resulting in $40 * 2 = 80$ pre-trained weights that incorporate the LoRA architecture.

During the learning of the t -th new task, O-LoRA updates the parameters $\mathbf{A}_t \in \mathbb{R}^{5120 \times r}$ and $\mathbf{B}_t \in \mathbb{R}^{r \times 5120}$, resulting in $5120 * r * 80 + r * 5120 * 80 = 819200r$ trainable parameters. When $r = 4$, the number of trainable parameters in O-LoRA is $819200 * 4 = 3276800 = 3.28\text{M}$. InfLoRA only updates the parameters $\mathbf{A}_t \in \mathbb{R}^{5120 \times r}$, resulting in $5120 * r * 80 = 409600r$ trainable parameters. When $r = 4$, the number of trainable parameters in InfLoRA is $409600 * 4 = 1638400 = 1.64\text{M}$.

GainLoRA introduces a new gating module $g_t(\cdot)$ with parameters $\mathbf{G}_{t,1} \in \mathbb{R}^{50 \times 5120}$, $\mathbf{G}_{t,2} \in \mathbb{R}^{5120 \times 50}$ and $\mathbf{G}_{t,3} \in \mathbb{R}^{1 \times 5120}$. Therefore, the number of trainable parameters in GainLoRA (O-LoRA) is $3276800 + 5120 * 50 + 5120 * 50 + 5120 = 3793920 = 3.79\text{M}$. The number of trainable parameters in GainLoRA (InfLoRA) is $1638400 + 5120 * 50 + 5120 * 50 + 5120 = 2155520 = 2.16\text{M}$.

Table 8: FLOPs and MACs for different models.

	Method	Input Shape (batch,length)	FLOPs (G)	MACs (G)
T5-Large	Original	(1,128)	194.25	97.1
	GainLoRA (O-LoRA)	(1,128)	198.79	99.37
	GainLoRA (InfLoRA)	(1,128)	198.79	99.37
T5-XL	Original	(1,128)	751.7	375.78
	GainLoRA (O-LoRA)	(1,128)	763.03	381.45
	GainLoRA (InfLoRA)	(1,128)	763.03	381.45
Llama-2-7B	Original	(1,128)	1701.07	850.5
	GainLoRA (O-LoRA)	(1,128)	1709.14	854.53
	GainLoRA (InfLoRA)	(1,128)	1709.14	854.53
Llama-2-13B	Original	(1,128)	3291.66	1645.79
	GainLoRA (O-LoRA)	(1,128)	3304.26	1652.09
	GainLoRA (InfLoRA)	(1,128)	3304.26	1652.09

C More Experimental Results

C.1 Discussing Computational Costs Introduced by GainLoRA

Existing methods, such as O-LoRA and InfLoRA, adopt the expandable LoRA architecture shown in Figure 1 (a) and fix the integration coefficients $\{a_i\}_{i=1}^T$ to 1, allowing the model to merge the expanded LoRA branches into the pre-trained matrix at inference time, thereby avoiding additional computational costs. However, when using our gating module to integrate different LoRA branches, the LoRA branches cannot be merged into the pre-trained matrix at inference time, which introduces additional computational costs. Nevertheless, we demonstrate that these computational costs are minimal compared to the computational cost of the original language models (LMs).

Table 8 compares the floating-point operations (FLOPs) and multiply-add operations (MACs) during inference for different models with and without GainLoRA. The computation of FLOPs and MACs follows the existing project calcflops [65]. Here, ‘‘Original’’ denotes the original LMs without any LoRA adaptation. Methods such as O-LoRA and InfLoRA avoid additional computational costs by merging their LoRA branches into the original weights during inference, resulting in FLOPs and MACs identical to the original LMs. Despite introducing additional FLOPs and MACs compared to the original LMs, GainLoRA maintains minimal computational overhead relative to the original LMs.

C.2 Additional Computation Introduced by Subspace Construction

The memory and computational overhead of subspace construction in GainLoRA is minimal due to the small size of the gating module (only 3 layers, see B.4). We provide detailed analyses below.

Memory The number of orthogonal bases stored for each subspace does not exceed its dimension. For T5-Large, the dimensions of the three subspaces are 1024, 100, and 1024, respectively. This results in a worst-case memory of less than 0.3% of the total model parameters $((2 * 1024^2 + 100^2)/(T5\text{-Large's params}) < 0.3\%)$. Similar estimates yield 0.07%, 0.5%, and 0.4% for T5-XL, Llama-2-7B, and Llama-2-13B, respectively. Since this calculation represents a rough upper bound, the actual memory is even lower.

Computational Overhead The computational overhead for subspace construction requires a single forward pass over the task dataset and SVD on the feature matrices of the gating module.

Assuming a single forward pass over the task dataset requires A FLOPs. For T5-Large, training a task for 100 epochs needs 100 forward and backward passes. Since a single backward pass has roughly $2A$ FLOPs, the total FLOPs are $500A$. Thus, a single forward pass for subspace construction accounts for only $1/500=0.2\%$ of total computation. Similar estimates yield 0.2%, 0.4%, and 0.4% for T5-XL, Llama-2-7B, and Llama-2-13B, respectively.

GPM requires performing SVD on matrix $H_l H_l^T \in \mathbb{R}^{d_l \times d_l}$, where H_l is the feature matrix in the l -th layer of gating module. Based on existing conclusions [52], the FLOPs for SVD on HH^T is less than $10d_l^3$. For T5-Large ($d_1 = d_3 = 1024$ and $d_2 = 100$), this results in $10 * (2 * 1024^3 + 100^3) <$

Table 9: Results with standard deviation on different task sequences using T5-large model.

Method	Order 1		Order 2		Order 3		Order 4	
	AP \uparrow	FT \downarrow	AP \uparrow	FT \downarrow	AP \uparrow	FT \downarrow	AP \uparrow	FT \downarrow
MIGU+FT [10]	-	-	-	-	71.30 \pm 1.85	11.39 \pm 1.92	69.05 \pm 0.71	14.06 \pm 0.86
SeqLoRA	7.30 \pm 1.12	47.60 \pm 0.94	7.03 \pm 0.49	47.97 \pm 0.07	49.46 \pm 2.42	27.60 \pm 4.09	33.81 \pm 0.01	45.53 \pm 1.60
IncLoRA [19]	12.33 \pm 0.56	41.93 \pm 0.17	16.65 \pm 0.91	36.56 \pm 1.30	61.19 \pm 0.85	13.63 \pm 1.27	62.46 \pm 0.34	15.92 \pm 0.46
C-LoRA [47]	22.69 \pm 0.01	24.25 \pm 0.90	32.81 \pm 0.64	11.60 \pm 0.23	66.83 \pm 0.56	8.64 \pm 0.32	61.86 \pm 1.77	14.18 \pm 1.50
O-LoRA [57]	26.37 \pm 2.27	19.15 \pm 2.15	32.83 \pm 0.25	11.99 \pm 0.38	70.98 \pm 1.74	3.69 \pm 0.53	71.21 \pm 0.33	4.03 \pm 1.00
GainLoRA (O-LoRA)	47.84\pm0.16	2.26\pm0.06	46.84\pm0.11	2.91 \pm 0.13	73.37 \pm 0.01	3.02 \pm 0.81	76.01 \pm 0.49	2.49\pm0.12
InfLoRA [30]	39.78 \pm 0.57	7.64 \pm 0.54	39.57 \pm 0.94	8.93 \pm 0.37	75.15 \pm 0.06	4.19 \pm 0.13	75.79 \pm 0.56	3.47 \pm 0.45
GainLoRA (InfLoRA)	46.21 \pm 0.05	2.40 \pm 0.24	46.44 \pm 0.41	2.61\pm0.25	78.01\pm0.26	0.77\pm0.01	77.54\pm0.23	1.25 \pm 0.10

Table 10: The overall results on different task sequences with T5-XL model.

Method	Order 1		Order 2		Order 3		Order 4	
	AP \uparrow	FT \downarrow	AP \uparrow	FT \downarrow	AP \uparrow	FT \downarrow	AP \uparrow	FT \downarrow
O-LoRA [57]	36.50 \pm 4.29	11.42 \pm 5.30	40.64 \pm 1.09	6.37 \pm 0.66	73.77 \pm 1.14	2.70 \pm 0.54	76.19 \pm 0.49	3.56 \pm 0.40
GainLoRA (O-LoRA)	50.10\pm0.22	3.21 \pm 0.32	49.86 \pm 0.06	3.04 \pm 0.13	78.41 \pm 0.50	2.59 \pm 0.56	77.21 \pm 0.19	3.30 \pm 0.34
InfLoRA [30]	45.61 \pm 1.28	5.60 \pm 1.35	45.85 \pm 0.10	5.10 \pm 0.32	80.22 \pm 0.04	2.09 \pm 0.11	79.43 \pm 0.03	1.71 \pm 0.09
GainLoRA (InfLoRA)	50.06 \pm 0.11	1.86\pm0.28	50.26\pm0.14	2.64\pm0.41	81.22\pm0.11	0.58\pm0.01	80.30\pm0.11	0.75\pm0.15

30GFLOPs, which is negligible compared to a single forward pass with sequence length 128 (see Table 8). Similar calculations give the same conclusion for T5-XL, Llama-2-7B, and Llama-2-13B.

C.3 Results with standard deviation

Table 9, Table 10 and Table 11 report the results with standard deviation.

Table 11: The overall results on different task sequences with Llama-2-7B and Llama-2-13B.

Method	Llama-2-7B				Llama-2-13B			
	Order 1		Order 2		Order 1		Order 2	
	AP \uparrow	FT \downarrow	AP \uparrow	FT \downarrow	AP \uparrow	FT \downarrow	AP \uparrow	FT \downarrow
O-LoRA [57]	39.37 \pm 0.24	15.84 \pm 0.58	37.55 \pm 0.70	20.23 \pm 0.20	43.92 \pm 0.42	14.15 \pm 0.35	40.05 \pm 0.46	19.53 \pm 0.50
GainLoRA (O-LoRA)	51.10 \pm 0.91	4.96 \pm 0.56	51.14\pm1.01	5.57 \pm 0.65	52.47 \pm 0.24	4.78 \pm 0.27	51.68 \pm 0.63	5.86 \pm 0.44
InfLoRA [30]	42.93 \pm 0.77	11.23 \pm 0.24	39.94 \pm 0.30	15.00 \pm 0.51	43.64 \pm 0.02	14.85 \pm 0.31	45.74 \pm 0.81	10.61 \pm 0.09
GainLoRA (InfLoRA)	51.27\pm0.01	2.84\pm0.11	50.17 \pm 0.32	4.71\pm0.22	53.64\pm0.81	2.87\pm0.05	52.46\pm0.50	4.90\pm0.30

C.4 Varying the Architecture of Gating Module

C.4.1 Varying Function $f(\cdot)$ in Gating Module

To implement our method, we define function $f(\cdot)$ as (7). Here, we vary the formula of function $f(\cdot)$ as the following two functions:

$$\min\{|b|, 1\}, |\sin(\frac{\pi b}{2})|. \quad (21)$$

Clearly, these two functions map real values among $[0, 1]$ and satisfy $f(0) = 0$. Table 12 shows the results. As we can see, when changing the formula of $f(\cdot)$, GainLoRA also improves the performance of O-LoRA and InfLoRA.

C.4.2 Varying the Shapes of Weights in Gating Module

In this section, we vary the shapes of the weights in the gating modules with T5-Large. Specifically, we set the weights $\mathbf{G}_{i,1} \in \mathbb{R}^{d_h \times 1024}$ and $\mathbf{G}_{i,2} \in \mathbb{R}^{1024 \times d_h}$ in each gating module $g_i(\cdot)$ and vary d_h over $\{50, 100, 200\}$. Figure 4 (a) and Figure 4 (b) show the results. As we can see, when increasing d_h , the performance of GainLoRA remains relatively stable, indicating that our method is robust to the shape of the weights in the gating module. Note that the number of trainable parameters increases as d_h increases.

Table 12: Varying the function $f(\cdot)$ in GainLoRA on different task sequences with T5-large model.

Method	Order 1		Order 2	
	AP \uparrow	FT \downarrow	AP \uparrow	FT \downarrow
GainLoRA (InfLoRA) ($f(b) = 2\text{sigmoid}(b) - 1 $)	46.21 \pm 0.05	2.40 \pm 0.24	46.44\pm0.41	2.61 \pm 0.25
GainLoRA (InfLoRA) ($f(b) = \min\{ b , 1\}$)	45.05 \pm 0.32	2.07 \pm 0.24	45.00 \pm 0.20	1.74\pm0.44
GainLoRA (InfLoRA) ($f(b) = \sin(\frac{\pi b}{2}) $)	47.48\pm0.03	1.21\pm0.52	45.03 \pm 0.67	2.37 \pm 0.34
InfLoRA	39.78 \pm 0.57	7.64 \pm 0.54	39.57 \pm 0.94	8.93 \pm 0.37
GainLoRA (O-LoRA) ($f(b) = 2\text{sigmoid}(b) - 1 $)	47.84 \pm 0.16	2.26\pm0.06	46.84 \pm 0.11	2.91\pm0.13
GainLoRA (O-LoRA) ($f(b) = \min\{ b , 1\}$)	49.62\pm0.57	2.83 \pm 0.73	48.62\pm0.47	3.74 \pm 0.02
GainLoRA (O-LoRA) ($f(b) = \sin(\frac{\pi b}{2}) $)	48.49 \pm 0.92	3.84 \pm 0.54	47.20 \pm 0.85	4.69 \pm 0.65
O-LoRA	26.37 \pm 2.27	19.15 \pm 2.15	32.83 \pm 0.25	11.99 \pm 0.38

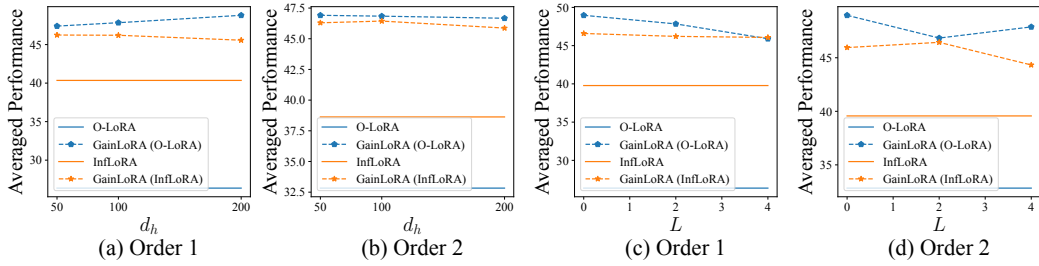


Figure 4: (a) and (b) show the variation of our methods’ performance with the shapes of the weights in the gating module. (c) and (d) show the variation of our methods’ performance with the Layers of the gating module.

C.4.3 Varying the Layers of Gating Module

In this section, we vary the layers of the gating modules with T5-Large. Specifically, we vary across $\{0, 2, 4\}$. when $L = 0$, there is only one layer with $\mathbf{G}_{i,1} \in \mathcal{R}^{1 \times 1024}$ in each gating module $g_i(\cdot)$. When $L = 2$, there are three layers with $\mathbf{G}_{i,1} \in \mathcal{R}^{100 \times 1024}$, $\mathbf{G}_{i,2} \in \mathcal{R}^{1024 \times 100}$ and $\mathbf{G}_{i,3} \in \mathcal{R}^{1 \times 1024}$. When $L = 4$, there are 5 layers with $\mathbf{G}_{i,1} \in \mathcal{R}^{100 \times 1024}$, $\mathbf{G}_{i,2} \in \mathcal{R}^{1024 \times 100}$, $\mathbf{G}_{i,3} \in \mathcal{R}^{100 \times 1024}$, $\mathbf{G}_{i,4} \in \mathcal{R}^{1024 \times 100}$, and $\mathbf{G}_{i,5} \in \mathcal{R}^{1 \times 1024}$ in each gating module. Figure 4 (c) and Figure 4 (d) show the results. As we can see, when increasing the layers of gating modules, the performance of GainLoRA remains relatively stable, indicating that our method is robust to the layers of the gating module. Note that the number of trainable parameters increases as the number of layers in gating modules increases.

C.5 Varying Ranks in LoRA Branches

In this section, we vary the rank of LoRA branches across $\{2, 4, 8\}$ with T5-Large. Figure 5 shows the results. As shown, when the rank of LoRA branches increases, the performance of GainLoRA remains relatively stable. Note that the number of trainable parameters increases as the rank of LoRA branches increases.

C.6 Adopting Other Update Strategies for the New LoRA Branch

Our GainLoRA does not impose specific update strategies for the new LoRA branches. In this work, we adopt the same update strategies as the existing two methods, O-LoRA [57] and InfLoRA [30]. Related methods, such as IncLoRA [19] and C-LoRA [47], also adopt the expandable LoRA architecture illustrated in Figure 1 (a) and fix all integration coefficients $\{a_i\}_{i=1}^T$ to 1. Our method GainLoRA can also adopt their update strategies for the new LoRA branch. Table 13 presents the results, demonstrating that GainLoRA further improves the performance of these two methods.

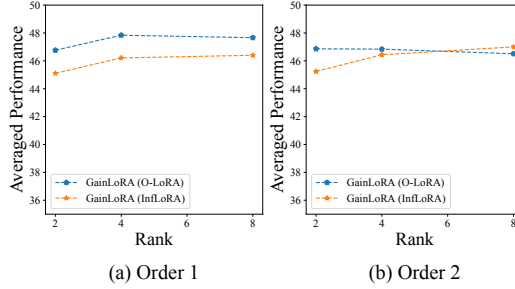


Figure 5: The variation of our methods’ performance with the Layers of the gating module.

Table 13: The overall results on different task sequences with T5-large model.

Method	Order 1		Order 2	
	AP↑	FT↓	AP↑	FT↓
IncLoRA	12.33±0.56	41.93±0.17	16.65±0.91	36.56±1.30
GainLoRA (IncLoRA)	47.82±0.08	3.73±0.25	45.42±1.19	5.83±1.53
C-LoRA	22.69±0.01	24.25±0.90	32.81±0.64	11.60±0.23
GainLoRA (C-LoRA)	49.24±0.21	2.94±0.41	46.23±0.61	6.05±0.51

C.7 Extending to the Rehearsal Setting

In this work, we focus on the non-rehearsal setting, where no real or synthetic samples from old tasks are available during the learning of a new task. In this section, we demonstrate that our method, GainLoRA, can also be extended to the rehearsal setting. Specifically, in the rehearsal setting, a set of samples \mathcal{N}_t containing real or synthetic samples from the previous $t - 1$ tasks is available while the model learns the t -th new task. In this case, the constraints introduced in Section 3.2.1 are no longer necessary, and we can optimize the following loss function:

$$\frac{1}{|\mathcal{D}_t|} \sum_{(\mathbf{x}_t, \mathbf{y}_t) \in \mathcal{D}_t} \sum_{j=1}^{|\mathbf{y}_t|} \log [P(y_{t,j} | \mathbf{x}_t, y_{t,1}, \dots, y_{t,j-1})] + \sum_{(\mathbf{x}, \mathbf{y}) \in \mathcal{N}_t} \log g_t(\mathbf{x}), \quad (22)$$

The second term in (22) minimizes the contribution from the new LoRA branch on old tasks.

We compare GainLoRA with SAPT-LoRA [71]. For a fair comparison, we use the same rehearsal dataset as SAPT-LoRA, generated using a trained generative model. As shown in Table 14, GainLoRA achieves comparable performance to SAPT-LoRA in the rehearsal setting. Note that SAPT-LoRA is specifically designed for the rehearsal setting and is not applicable to the non-rehearsal setting, which is considered in this work.

Table 14: The overall results on Order 1 in the rehearsal-setting.

	T5-Large		Llama-2-7B	
	AP↑	FT↓	AP↑	FT↓
SAPT-LoRA [71]	51.38±0.12	0.74±0.18	55.88±0.25	0.74±0.27
GainLoRA (InfLoRA) + Replay	51.62±0.56	0.08±0.10	55.93±0.69	0.95±0.39

C.8 Performance on the TRACE Benchmark

To further demonstrate our method’s effectiveness, we follow existing CL methods for LMs [16, 58] and conduct experiments on the TRACE dataset [58] with Llama-2-7B-Chat. The dataset comprises a diverse set of challenging instruction-tuned tasks, spanning multilingual comprehension, domain-specific knowledge, arithmetic reasoning, and coding. An overview of the tasks in TRACE is provided in Table 15.

Table 16 reports the average performance on the TRACE benchmark after sequentially learning all tasks. The results demonstrate that our method effectively mitigates catastrophic forgetting and outperforms existing baselines. This capability is crucial for real-world applications.

Table 15: The order of TRACE benchmark for experiments.

Benchmark	Task Sequence
TRACE Benchmark	C-STANCE → FOMC → MeetingBank → Py150 → ScienceQA → NumGLUE-cm → NUMGLUE-ds → 20Minuten

Table 16: TRACE benchmark performance using LLama-2-7B-Chat.

	AP↑	FT↓
O-LoRA [57]	41.04	8.05
GainLoRA (O-LoRA)	48.10	0.99
InfLoRA [30]	47.67	2.25
GainLoRA (InfLoRA)	49.15	0.89

Table 17: Comparison of general ability scores across six diverse evaluation tasks between the base LLaMA-2-7B chat model and different methods.

	PIQA	MMLU	GSM8K	BBH	BoolQA	TydiQA
O-LoRA [57]	72.85	32.87	13.42	35.10	56.88	19.48
GainLoRA (O-LoRA)	73.61	33.33	18.57	36.47	59.69	25.00
InfLoRA [30]	74.86	40.86	15.69	35.87	65.29	27.25
GainLoRA (InfLoRA)	75.24	44.25	21.30	37.44	68.81	27.84
Llama-2-7B-Chat	75.35	46.13	26.54	40.09	70.46	23.45

Retention of General Capabilities We also follow existing work [58] to explicitly evaluate the preservation of general abilities, such as instruction-following, after continual learning on the TRACE benchmark using different methods. Table 17 indicates that continual learning with different methods often leads to a degradation of general abilities. However, GainLoRA demonstrates a stronger ability to mitigate forgetting compared to other LoRA-based methods, including O-LoRA and InfLoRA.

C.9 Compared with More CL Methods in CV

Following many existing continual learning methods in NLP [71, 57, 16], this paper focuses on models based on next-token prediction, such as T5 [40] and LLaMA [51], which lack the [CLS] token used in ViT. Although many continual learning methods based on pre-trained models in computer vision [62, 63, 59, 53, 54, 48] cannot be directly applied to our setting, we adapt several of them to the T5 architecture to ensure a comprehensive comparison. Specifically, we select three representative methods from the vision domain, including L2P [63], DualPrompt [62], and CODA-Prompt [48]. These methods rely on the [CLS] token in ViT to retrieve prompts from a prompt pool for training and inference. Since T5 does not provide a [CLS] token, we instead use the mean representation of each input sequence as a query. We carefully tuned the learning rate, epochs, and their unique hyperparameters on the validation set. Table 18 presents the performance of these adapted methods on order 1 with T5. As shown, they perform significantly worse than our GainLoRA and exhibit noticeable forgetting.

Table 18: Compare with different methods on order 1 with T5 architecture.

	AP↑	FT↓
L2P [63]	14.59	24.70
DualPrompt [62]	11.77	12.95
CODA-Prompt [48]	10.80	16.15
GainLoRA (O-LoRA)	47.84	2.26
GainLoRA (InfLoRA)	46.21	2.40

References

- [1] Elahe Arani, Fahad Sarfraz, and Bahram Zonooz. Learning fast, learning slow: A general continual learning method based on complementary learning system. In *International Conference on Learning Representations*, 2022.

- [2] PENG Bohao, Zhuotao Tian, Shu Liu, Ming-Chang Yang, and Jiaya Jia. Scalable language model with generalized continual learning. In *International Conference on Learning Representations*, 2024.
- [3] Tom Brown, Benjamin Mann, Nick Ryder, Melanie Subbiah, Jared D Kaplan, Prafulla Dhariwal, Arvind Neelakantan, Pranav Shyam, Girish Sastry, Amanda Askell, et al. Language models are few-shot learners. *Advances in Neural Information Processing Systems*, pages 1877–1901, 2020.
- [4] Arslan Chaudhry, Naeemullah Khan, Puneet Dokania, and Philip Torr. Continual learning in low-rank orthogonal subspaces. *Advances in Neural Information Processing Systems*, pages 9900–9911, 2020.
- [5] Arslan Chaudhry, Marcus Rohrbach, Mohamed Elhoseiny, Thalaiyasingam Ajanthan, Puneet K Dokania, Philip HS Torr, and Marc’ Aurelio Ranzato. On tiny episodic memories in continual learning. *arXiv preprint arXiv:1902.10486*, 2019.
- [6] Kyunghyun Cho. On the properties of neural machine translation: Encoder-decoder approaches. *arXiv preprint arXiv:1409.1259*, 2014.
- [7] Aakanksha Chowdhery, Sharan Narang, Jacob Devlin, Maarten Bosma, Gaurav Mishra, Adam Roberts, Paul Barham, Hyung Won Chung, Charles Sutton, Sebastian Gehrmann, et al. Palm: Scaling language modeling with pathways. *Journal of Machine Learning Research*, pages 1–113, 2023.
- [8] Tri Dao. Flashattention-2: Faster attention with better parallelism and work partitioning. In *International Conference on Learning Representations*, 2024.
- [9] Cyprien de Masson d’Autume, Sebastian Ruder, Lingpeng Kong, and Dani Yogatama. Episodic memory in lifelong language learning. In *Advances in Neural Information Processing Systems*, pages 13122–13131, 2019.
- [10] Wenyu Du, Shuang Cheng, Tongxu Luo, Zihan Qiu, Zeyu Huang, Ka Chun Cheung, Reynold Cheng, and Jie Fu. Unlocking continual learning abilities in language models. In *Findings of the Conference on Empirical Methods in Natural Language Processing*, pages 6503–6522, 2024.
- [11] Stefan Elfving, Eiji Uchibe, and Kenji Doya. Sigmoid-weighted linear units for neural network function approximation in reinforcement learning. *Neural Networks*, pages 3–11, 2018.
- [12] Yujie Feng, Xu Chu, Yongxin Xu, Zexin Lu, Bo Liu, Philip S Yu, and Xiao-Ming Wu. Kif: Knowledge identification and fusion for language model continual learning. *arXiv preprint arXiv:2408.05200*, 2024.
- [13] Yujie Feng, Xu Chu, Yongxin Xu, Guangyuan Shi, Bo Liu, and Xiao-Ming Wu. Tasl: Continual dialog state tracking via task skill localization and consolidation. In *Proceedings of the Annual Meeting of the Association for Computational Linguistics*, pages 1266–1279, 2024.
- [14] Chin-Lun Fu, Zih-Ching Chen, Yun-Ru Lee, and Hung-Yi Lee. Adapterbias: Parameter-efficient token-dependent representation shift for adapters in nlp tasks. In *Findings of the Conference of the North American Chapter of the Association for Computational Linguistics*, pages 2608–2621, 2022.
- [15] Zeyu Han, Chao Gao, Jinyang Liu, Sai Qian Zhang, et al. Parameter-efficient fine-tuning for large models: A comprehensive survey. *arXiv preprint arXiv:2403.14608*, 2024.
- [16] Jinghan He, Haiyun Guo, Kuan Zhu, Zihan Zhao, Ming Tang, and Jinqiao Wang. Seekr: Selective attention-guided knowledge retention for continual learning of large language models. In *Proceedings of the Conference on Empirical Methods in Natural Language Processing*, pages 3254–3266, 2024.
- [17] Sepp Hochreiter and Jürgen Schmidhuber. Long short-term memory. *Neural Computation*, pages 1735–1780, 1997.

- [18] Neil Houlsby, Andrei Giurgiu, Stanislaw Jastrzebski, Bruna Morrone, Quentin De Laroussilhe, Andrea Gesmundo, Mona Attariyan, and Sylvain Gelly. Parameter-efficient transfer learning for nlp. In *Proceedings of the International Conference on Machine Learning*, pages 2790–2799, 2019.
- [19] Edward J Hu, Phillip Wallis, Zeyuan Allen-Zhu, Yuanzhi Li, Shean Wang, Lu Wang, Weizhu Chen, et al. Lora: Low-rank adaptation of large language models. In *International Conference on Learning Representations*, 2022.
- [20] Steven C. Y. Hung, Cheng-Hao Tu, Cheng-En Wu, Chien-Hung Chen, Yi-Ming Chan, and Chu-Song Chen. Compacting, picking and growing for unforgetting continual learning. In *Advances in Neural Information Processing Systems*, pages 13647–13657, 2019.
- [21] Sangwon Jung, Hongjoon Ahn, Sungmin Cha, and Taesup Moon. Continual learning with node-importance based adaptive group sparse regularization. *Advances in Neural Information Processing Systems*, pages 3647–3658, 2020.
- [22] James Kirkpatrick, Razvan Pascanu, Neil Rabinowitz, Joel Veness, Guillaume Desjardins, Andrei A Rusu, Kieran Milan, John Quan, Tiago Ramalho, Agnieszka Grabska-Barwinska, et al. Overcoming catastrophic forgetting in neural networks. *Proceedings of the National Academy of Sciences*, pages 3521–3526, 2017.
- [23] Minh Le, Huy Nguyen, Trang Nguyen, Trang Pham, Linh Ngo, Nhat Ho, et al. Mixture of experts meets prompt-based continual learning. *Advances in Neural Information Processing Systems*, pages 119025–119062, 2024.
- [24] Brian Lester, Rami Al-Rfou, and Noah Constant. The power of scale for parameter-efficient prompt tuning. In *Proceedings of the Conference on Empirical Methods in Natural Language Processing*, pages 3045–3059, 2021.
- [25] Xiang Lisa Li and Percy Liang. Prefix-tuning: Optimizing continuous prompts for generation. In *Proceedings of the Annual Meeting of the Association for Computational Linguistics*, pages 4582–4597, 2021.
- [26] Xilai Li, Yingbo Zhou, Tianfu Wu, Richard Socher, and Caiming Xiong. Learn to grow: A continual structure learning framework for overcoming catastrophic forgetting. In *Proceedings of the International Conference on Machine Learning*, pages 3925–3934, 2019.
- [27] Zhizhong Li and Derek Hoiem. Learning without forgetting. *IEEE transactions on pattern analysis and machine intelligence*, pages 2935–2947, 2017.
- [28] Yan-Shuo Liang and Wu-Jun Li. Adaptive plasticity improvement for continual learning. In *Proceedings of the IEEE/CVF Conference on Computer Vision and Pattern Recognition*, pages 7816–7825, 2023.
- [29] Yan-Shuo Liang and Wu-Jun Li. Loss decoupling for task-agnostic continual learning. In *Advances in Neural Information Processing Systems*, 2023.
- [30] Yan-Shuo Liang and Wu-Jun Li. Inflora: Interference-free low-rank adaptation for continual learning. In *Proceedings of the IEEE/CVF Conference on Computer Vision and Pattern Recognition*, pages 23638–23647, 2024.
- [31] Chin-Yew Lin. Rouge: A package for automatic evaluation of summaries. In *Text Summarization Branches Out*, pages 74–81, 2004.
- [32] David Lopez-Paz and Marc’ Aurelio Ranzato. Gradient episodic memory for continual learning. In *Advances in Neural Information Processing Systems*, pages 6470–6479, 2017.
- [33] Ilya Loshchilov and Frank Hutter. Decoupled weight decay regularization. In *International Conference on Learning Representations*, 2019.
- [34] Yun Luo, Zhen Yang, Fandong Meng, Yafu Li, Jie Zhou, and Yue Zhang. An empirical study of catastrophic forgetting in large language models during continual fine-tuning. *arXiv preprint arXiv:2308.08747*, 2023.

- [35] Rabeeh Karimi Mahabadi, James Henderson, and Sebastian Ruder. Compacter: Efficient low-rank hypercomplex adapter layers. In *Advances in Neural Information Processing Systems*, pages 1022–1035, 2021.
- [36] Mark D McDonnell, Dong Gong, Amin Parvaneh, Ehsan Abbasnejad, and Anton Van den Hengel. Ranpac: Random projections and pre-trained models for continual learning. *Advances in Neural Information Processing Systems*, pages 12022–12053, 2023.
- [37] Long Ouyang, Jeffrey Wu, Xu Jiang, Diogo Almeida, Carroll Wainwright, Pamela Mishkin, Chong Zhang, Sandhini Agarwal, Katarina Slama, Alex Ray, et al. Training language models to follow instructions with human feedback. *Advances in Neural Information Processing Systems*, pages 27730–27744, 2022.
- [38] German I Parisi, Ronald Kemker, Jose L Part, Christopher Kanan, and Stefan Wermter. Continual lifelong learning with neural networks: A review. *Neural Networks*, pages 54–71, 2019.
- [39] Chengwei Qin and Shafiq R. Joty. LFPT5: A unified framework for lifelong few-shot language learning based on prompt tuning of T5. In *International Conference on Learning Representations*, 2022.
- [40] Colin Raffel, Noam Shazeer, Adam Roberts, Katherine Lee, Sharan Narang, Michael Matena, Yanqi Zhou, Wei Li, and Peter J Liu. Exploring the limits of transfer learning with a unified text-to-text transformer. *Journal of Machine Learning Research*, pages 1–67, 2020.
- [41] Jeff Rasley, Samyam Rajbhandari, Olatunji Ruwase, and Yuxiong He. Deepspeed: System optimizations enable training deep learning models with over 100 billion parameters. In *Proceedings of the International Conference on Knowledge Discovery & Data Mining*, pages 3505–3506, 2020.
- [42] Anastasia Razdaibiedina, Yuning Mao, Rui Hou, Madian Khabza, Mike Lewis, and Amjad Almahairi. Progressive prompts: Continual learning for language models. In *International Conference on Learning Representations*, 2023.
- [43] Andrei A Rusu, Neil C Rabinowitz, Guillaume Desjardins, Hubert Soyer, James Kirkpatrick, Koray Kavukcuoglu, Razvan Pascanu, and Raia Hadsell. Progressive neural networks. *arXiv preprint arXiv:1606.04671*, 2016.
- [44] Gobinda Saha, Isha Garg, and Kaushik Roy. Gradient projection memory for continual learning. In *International Conference on Learning Representations*, 2021.
- [45] Haizhou Shi, Zihao Xu, Hengyi Wang, Weiyi Qin, Wenyuan Wang, Yibin Wang, and Hao Wang. Continual learning of large language models: A comprehensive survey. *arXiv preprint arXiv:2404.16789*, 2024.
- [46] James Seale Smith, Paola Cascante-Bonilla, Assaf Arbelle, Donghyun Kim, Rameswar Panda, David Cox, Diyi Yang, Zsolt Kira, Rogerio Feris, and Leonid Karlinsky. Construct-vl: Data-free continual structured vl concepts learning. In *Proceedings of the IEEE/CVF Conference on Computer Vision and Pattern Recognition*, pages 14994–15004, 2023.
- [47] James Seale Smith, Yen-Chang Hsu, Lingyu Zhang, Ting Hua, Zsolt Kira, Yilin Shen, and Hongxia Jin. Continual diffusion: Continual customization of text-to-image diffusion with c-lora. *Transactions on Machine Learning Research*, 2024.
- [48] James Seale Smith, Leonid Karlinsky, Vyshnavi Gutta, Paola Cascante-Bonilla, Donghyun Kim, Assaf Arbelle, Rameswar Panda, Rogerio Feris, and Zsolt Kira. Coda-prompt: Continual decomposed attention-based prompting for rehearsal-free continual learning. In *Proceedings of the IEEE/CVF Conference on Computer Vision and Pattern Recognition*, pages 11909–11919, 2023.
- [49] Fan-Keng Sun, Cheng-Hao Ho, and Hung-Yi Lee. Lamol: Language modeling for lifelong language learning. In *International Conference on Learning Representations*, 2020.

- [50] Hugo Touvron, Thibaut Lavril, Gautier Izacard, Xavier Martinet, Marie-Anne Lachaux, Timothée Lacroix, Baptiste Rozière, Naman Goyal, Eric Hambro, Faisal Azhar, et al. Llama: Open and efficient foundation language models. *arXiv preprint arXiv:2302.13971*, 2023.
- [51] Hugo Touvron, Louis Martin, Kevin Stone, Peter Albert, Amjad Almahairi, Yasmine Babaei, Nikolay Bashlykov, Soumya Batra, Prajjwal Bhargava, Shruti Bhosale, et al. Llama 2: Open foundation and fine-tuned chat models. *arXiv preprint arXiv:2307.09288*, 2023.
- [52] Lloyd N Trefethen and David Bau. *Numerical linear algebra*. SIAM, 2022.
- [53] Liyuan Wang, Jingyi Xie, Xingxing Zhang, Mingyi Huang, Hang Su, and Jun Zhu. Hierarchical decomposition of prompt-based continual learning: Rethinking obscured sub-optimality. *Advances in Neural Information Processing Systems*, pages 69054–69076, 2023.
- [54] Liyuan Wang, Jingyi Xie, Xingxing Zhang, Hang Su, and Jun Zhu. Hide-pet: Continual learning via hierarchical decomposition of parameter-efficient tuning. *arXiv e-prints*, 2024.
- [55] Liyuan Wang, Xingxing Zhang, Hang Su, and Jun Zhu. A comprehensive survey of continual learning: Theory, method and application. *IEEE Transactions on Pattern Analysis and Machine Intelligence*, pages 5362–5383, 2024.
- [56] Shipeng Wang, Xiaorong Li, Jian Sun, and Zongben Xu. Training networks in null space of feature covariance for continual learning. In *Proceedings of the IEEE/CVF Conference on Computer Vision and Pattern Recognition*, pages 184–193, 2021.
- [57] Xiao Wang, Tianze Chen, Qiming Ge, Han Xia, Rong Bao, Rui Zheng, Qi Zhang, Tao Gui, and Xuan-Jing Huang. Orthogonal subspace learning for language model continual learning. In *Findings of the Conference on Empirical Methods in Natural Language Processing*, pages 10658–10671, 2023.
- [58] Xiao Wang, Yuansen Zhang, Tianze Chen, Songyang Gao, Senjie Jin, Xianjun Yang, Zhiheng Xi, Rui Zheng, Yicheng Zou, Tao Gui, et al. Trace: A comprehensive benchmark for continual learning in large language models. *arXiv preprint arXiv:2310.06762*, 2023.
- [59] Yabin Wang, Zhiwu Huang, and Xiaopeng Hong. S-prompts learning with pre-trained transformers: An occam’s razor for domain incremental learning. *Advances in Neural Information Processing Systems*, pages 5682–5695, 2022.
- [60] Yizhong Wang, Swaroop Mishra, Pegah Alipoormolabashi, Yeganeh Kordi, Amirreza Mirzaei, Atharva Naik, Arjun Ashok, Arut Selvan Dhanasekaran, Anjana Arunkumar, David Stap, Eshaan Pathak, Giannis Karamanolakis, Haizhi Gary Lai, Ishan Purohit, Ishani Mondal, Jacob Anderson, Kirby Kuznia, Krma Doshi, Kuntal Kumar Pal, Maitreya Patel, Mehrad Moradshahi, Mihir Parmar, Mirali Purohit, Neeraj Varshney, Phani Rohitha Kaza, Pulkit Verma, Ravsehaj Singh Puri, Rushang Karia, Savan Doshi, Shailaja Keyur Sampat, Siddhartha Mishra, Sujana Reddy A, Sumanta Patro, Tanay Dixit, and Xudong Shen. Super-naturalinstructions: Generalization via declarative instructions on 1600+ NLP tasks. In *Proceedings of the Conference on Empirical Methods in Natural Language Processing*, pages 5085–5109, 2022.
- [61] Zhicheng Wang, Yufang Liu, Tao Ji, Xiaoling Wang, Yuanbin Wu, Congcong Jiang, Ye Chao, Zhencong Han, Ling Wang, Xu Shao, et al. Rehearsal-free continual language learning via efficient parameter isolation. In *Proceedings of the Annual Meeting of the Association for Computational Linguistics*, pages 10933–10946, 2023.
- [62] Zifeng Wang, Zizhao Zhang, Sayna Ebrahimi, Ruoxi Sun, Han Zhang, Chen-Yu Lee, Xiaoqi Ren, Guolong Su, Vincent Perot, Jennifer Dy, et al. Dualprompt: Complementary prompting for rehearsal-free continual learning. In *Proceedings of the European Conference on Computer Vision*, pages 631–648, 2022.
- [63] Zifeng Wang, Zizhao Zhang, Chen-Yu Lee, Han Zhang, Ruoxi Sun, Xiaoqi Ren, Guolong Su, Vincent Perot, Jennifer Dy, and Tomas Pfister. Learning to prompt for continual learning. In *Proceedings of the IEEE/CVF Conference on Computer Vision and Pattern Recognition*, pages 139–149, 2022.

- [64] Jason Wei, Maarten Bosma, Vincent Zhao, Kelvin Guu, Adams Wei Yu, Brian Lester, Nan Du, Andrew M Dai, and Quoc V Le. Finetuned language models are zero-shot learners. In *International Conference on Learning Representations*, 2022.
- [65] X Ye. calflops: a flops and params calculate tool for neural networks in pytorch framework, 2023.
- [66] Elad Ben Zaken, Yoav Goldberg, and Shauli Ravfogel. Bitfit: Simple parameter-efficient fine-tuning for transformer-based masked language-models. In *Proceedings of the Annual Meeting of the Association for Computational Linguistics*, pages 1–9, 2022.
- [67] Gengwei Zhang, Liyuan Wang, Guoliang Kang, Ling Chen, and Yunchao Wei. Slca: Slow learner with classifier alignment for continual learning on a pre-trained model. In *Proceedings of the IEEE/CVF International Conference on Computer Vision*, pages 19148–19158, 2023.
- [68] Qingru Zhang, Minshuo Chen, Alexander Bukharin, Pengcheng He, Yu Cheng, Weizhu Chen, and Tuo Zhao. Adaptive budget allocation for parameter-efficient fine-tuning. In *The Eleventh International Conference on Learning Representations*, 2023.
- [69] Susan Zhang, Stephen Roller, Naman Goyal, Mikel Artetxe, Moya Chen, Shuohui Chen, Christopher Dewan, Mona Diab, Xian Li, Xi Victoria Lin, et al. Opt: Open pre-trained transformer language models. *arXiv preprint arXiv:2205.01068*, 2022.
- [70] Linglan Zhao, Xuerui Zhang, Ke Yan, Shouhong Ding, and Weiran Huang. SAFE: slow and fast parameter-efficient tuning for continual learning with pre-trained models. In *Advances in Neural Information Processing Systems*, 2024.
- [71] Weixiang Zhao, Shilong Wang, Yulin Hu, Yanyan Zhao, Bing Qin, Xuanyu Zhang, Qing Yang, Dongliang Xu, and Wanxiang Che. Sapt: A shared attention framework for parameter-efficient continual learning of large language models. In *Proceedings of the Annual Meeting of the Association for Computational Linguistics*, pages 11641–11661, 2024.